EPA

United States
Environmental Protection
Agency

Mg

SF₆ Emission Reduction
Partnership for the Magnesium Industry

Characterization of Cover Gas and Byproduct Emissions from Secondary Magnesium Ingot Casting

Office of Air and Radiation
Office of Atmospheric Programs, Climate Change Division

EPA 430-R-08-008

Characterization of Cover Gas and Byproduct Emissions from Secondary Magnesium Ingot Casting

Scott C. Bartos
U.S. Environmental Protection Agency
Climate Change Division
1200 Pennsylvania Avenue, NW (6202J)
Washington, DC 20460

October 2008

Table of Contents

List of Tables

List of Figures

Acknowledgements

Executive Summary

This measurement study was conducted to evaluate the greenhouse gas (GHG) emissions and occupational exposure associated with three cover gas technologies used in a magnesium alloy ingot casting machine. Sulfur hexafluoride (SF_6) is widely used for the protection from oxidation of molten magnesium; but with the goal of eliminating the use of SF_6 in this application by 2010, the magnesium industry and U.S. Environmental Protection Agency (EPA) have been evaluating the use of alternative gases. This study expands upon previous research by continuously monitoring multiple sample points and by testing cover gas mixtures in an ingot casting hood environment – previous research used single sampling points and examined die casting holding furnaces.[1] This study examined the use of SF_6, pentafluoroethylhepafluoro-isopropylketone (Novec™ 612), and sulfur dioxide (SO_2) on an ingot casting machine located at a Magnesium Refining Technologies (MagReTech) facility located in Bellevue, Ohio. Process and machine operating parameters were maintained at similar levels when each cover gas mixture was evaluated. Each cover gas mixture was injected into the ingot casting hood and sampled from the hot and cold zones of the casting hood to characterize emissions and byproducts as the cover gases interact with the magnesium melt surface and undergo thermo-degradation. The results reported are from measurements taken from multiple points inside the casting hood, and from an ambient air sampling point in the casting hood operator room. Results are presented for four sample points: the upstream sampling point in the hot zone (hu), the downstream sampling point in the hot zone (hd), the upstream sampling point in the cold zone (cu), and the downstream sampling point in the cold zone (cd). Table ES-1 summarizes some of the details and results from the ingot casting hood component of the study. Measurements were conducted using slightly varied mixtures of each cover gas. The cover gas destruction rates listed in Table ES-1 have been corrected for dilution effects.[2]

SF_6/SO_2 with CDA/CO_2 Carrier Gas

The only destruction byproduct measured while using SF_6/SO_2 with clean dry air (CDA)/CO_2 as a cover gas was HF, with concentrations ranging from 0.02 to 0.37 ppmv over three different testing periods. Other byproducts, including COS, CS_2, H_2S, and H_2SO_4, (see Table 2-1 for a listing of chemical formulas and compound names) were not analytically detected. CH_4 was observed at average concentrations of 2.6 to 82.8 ppmv during the three tests; the normal ambient air concentration of CH_4 is ~2 ppmv. The high concentration of CH_4 is most likely due to the periodic use of to natural gas burners to preheat the ingot molds, therefore CH_4

---

[1] US EPA. *Characterization of Emissions and Occupational Exposure Associated with Five Cover Gas Technologies for Magnesium Die Casting*, EPA 430-R-07-008, August 2007.
[2] The term destruction is utilized throughout the remainder of this report to represent the thermo-degradation and disassociation of the cover gas agent resulting in byproduct formation and melt protection.

measured in the ingot casting hood was assumed to originate from fugitive emissions in the facility rather than process emissions associated with cover gas application.

MTG-Shield™ using Novec™ 612 with CDA/CO$_2$ Carrier Gas

The only destruction byproducts measured while running MTG-Shield™ using Novec™ 612 with CDA/CO$_2$ as a cover gas were HF and CHF$_3$. COF$_2$, CF$_4$, C$_2$F$_6$, C$_3$F$_8$, OF$_2$, CH$_2$O$_2$, and H$_2$CO were expected byproducts that were not analytically detected. HF was detected at concentrations ranging from 0.05 to 1.5 ppmv for the three Novec™ 612 testing periods. CHF$_3$ was twice detected at the downstream sampling point in the hot zone at concentrations ranging from 0.15 to 0.30 ppmv. Perfluoroisobutylene (PFIB), an occupational hazard and primary byproduct of concern, was monitored for, but not detected during this study.

SO$_2$ with CDA Carrier Gas

There were no destruction byproducts detected that could be attributed to the SO$_2$ with CDA cover gas mixture. The only detectable compounds were ambient air and combustion-related compounds (H$_2$O, CO, CO$_2$, and CH$_4$). Methane was detected at average concentrations ranging from 3.2 to 3.6 ppmv. Sulfuric acid and H$_2$S were not measured at concentrations above their minimum detection limits within the ingot casting hood.

Observed Percent Destruction for Cover Gases

Table ES-1 lists the destruction estimates for all cover gases examined. The destruction estimates, which are corrected for dilution effects (i.e., the effects of air ingression into the ingot casting hood), are calculated as the percent difference between the expected dilution corrected delivery concentration and the measured concentration in the casting area. Average destruction estimates for Novec™ 612 and SF$_6$ were on the order of four percent and three percent, respectively. In comparison, destruction estimates for SO$_2$ were on the order of 39 percent for this study. It should be noted that high levels of dilution found in this study and associated uncertainty resulted in calculated destruction rates for some tests being unreasonable (i.e., negative) and these values were treated as zero destruction results.

The destruction rates estimated for SF$_6$ in this study were significantly lower than what was estimated during previous research evaluating die casting holding furnaces (on the order of 20 to 30 percent). This is likely due to the much higher levels of dilution and reduced thermo-chemical intensity of the casting hood environment.

Table ES-1. Cover Gas Average Concentrations and Observed Destruction

Test # (site)	Cover Gas Mixture Components	Time	Cover Gas Mixture Flow[a] (lpm)	Cover Gas Delivery Conc.[b] (ppmv)	Cover Gas Dil. Corr. Conc.[c] (ppmv)	Cover Gas Measured Conc. (ppmv)	Cover Gas Destruction Factor (percent)
1hu	SF_6 / SO_2 / CDA / CO_2	1730-1930	270	10,675	1,459	1,407	4%
1cu	SF_6 / SO_2 / CDA / CO_2	1730-1930	135	10,675	624	572	8%
2hu	SF_6 / SO_2 / CDA / CO_2	1115-1345	198	7,554	1,285	1,251	3%
2cu	SF_6 / SO_2 / CDA / CO_2	1115-1345	99	7,554	490	456	7%
3hu	SF_6 / SO_2 / CDA / CO_2	0915-1200	270	8,463	954	1,232	≈0%
3cu	SF_6 / SO_2 / CDA / CO_2	0915-1200	135	8,463	479	640	≈0%
3hd	SF_6 / SO_2 / CDA / CO_2	0915-1200	270	8,463	301	424	≈0%
3cd	SF_6 / SO_2 / CDA / CO_2	0915-1200	135	8,463	212	333	≈0%
4hu	Novec™ 612 / CDA / CO_2	1500-1709	189	2,000	220	219	≈0%
4cu	Novec™ 612 / CDA / CO_2	1500-1709	95	2,000	76	77	≈0%
5hd	Novec™ 612 / CDA / CO_2	1710-1730	189	1,500	40	47	≈0%
5cd	Novec™ 612 / CDA / CO_2	1710-1730	95	1,500	30	27	10%
6hu	Novec™ 612 / CDA / CO_2	0915-1140	191	1,102	124	96	23%
6cu	Novec™ 612 / CDA / CO_2	0915-1140	96	1,102	62	161	≈0%
6hd	Novec™ 612 / CDA / CO_2	0915-1140	191	1,102	39	37	4%
6cd	Novec™ 612 / CDA / CO_2	0915-1140	96	1,102	28	74	≈0%
7hu	Novec™ 612 / CDA / CO_2	1420-1620	189	1,663	125	131	≈0%
7cu	Novec™ 612 / CDA / CO_2	1420-1620	95	1,663	241	228	5%
8hd	SO_2 / CDA	1340-1540	191	10,000	356	277	22%
8cd	SO_2 / CDA	1340-1540	95	10,000	250	128	49%
9hu	SO_2 / CDA	0740-1000	191	12,000	1353	946	30%
9cu	SO_2 / CDA	0740-1000	96	12,000	679	296	56%

[a] Approximate, estimated by reading flow rates on gas delivery manifold rotameters (uncalibrated). Two-thirds of the flow went to the hot zone and one third to the cold zone. Additional details on cover gas mixture can be found in Table 1-1.
[b] Measured directly at manifold; only for primary gases of concern (SF_6, Novec™ 612, and SO_2) for the three cover gas systems.
[c] Dilution corrected concentration based on dilution estimates in Chapter 4. These are the expected concentrations with no destruction occurring.

Occupational Exposure Monitoring

Since each cover gas used in this study can result in emissions that may be harmful to exposed workers, monitoring of the ambient air in the casting hood worker room was performed using another FTIR. This component of the study was especially relevant to SO_2 as well as the byproduct HF, due to their stringent occupational exposure limits. The breathing zone located near the worker responsible for skimming ingot surfaces was continuously monitored during the study. Table 3.5 lists the results for the occupational exposure monitoring performed during this study. On average, the only compound found in the worker room above detectable levels was SF_6, which was only present when the SF_6/SO_2 cover gas was being used. Sulfur dioxide,

Novec™ 612, and HF were not present in the worker room above detectable levels for any of the cover gas mixtures and SF_6 was not detected during the Novec™ 612 or SO_2 tests.[3]

Potential Climate Impact

A key factor in evaluating alternative cover gas compounds was their composite global warming potentials (GWPs) as compared to SF_6. Global warming potentials are based on the heat-absorbing capability and atmospheric lifetime of each gas relative to that of carbon dioxide. The GWP provides a construct for converting emissions of various gases into a common measure, denominated in carbon dioxide equivalents. For each cover gas compound and its applicable destruction byproducts, a composite global warming impact estimate was developed using the IPCC Fourth Assessment Report (AR4) GWP values.[4] The overall GWP-weighted gas emission rate for each cover gas regime was estimated using the measured average concentrations of each gas, their molecular weights, and the delivery cover gas flow rates. This resulted in a normalized CO_2 emission equivalent for each alternative cover gas that could be directly compared to the CO_2 emission equivalent of the existing SF_6/SO_2 system.

Based on this approach, results indicate that both the Novec™ 612 cover gas mixture and the SO_2 cover gas mixture have a GHG emission impact – weighted by cover gas flow – that is at least 99 percent lower than SF_6. Table ES-2 presents the results of the global warming potential analysis for the alternative cover gas mixtures examined in this experiment.

Table ES-2. Global Warming Potential of Alternative Cover Gas Mixtures

Cover Gas Mixture	GHG Emissions Relative to Existing SF_6 / SO_2 system (percent reduction)
Novec™ 612 / CDA / CO_2	>99%
SO_2 / CDA	>99%

---

[3] All applicable safety precautions (e.g., operational procedures) should be followed when using SO_2.
[4] IPCC, Climate Change 2007: The Scientific Basis. Intergovernmental Panel on Climate Change, 2007, Cambridge University Press. Cambridge, U.K.

1. Introduction

This report presents and interprets the results of a series of emission measurements taken of air-entrained cover gas mixtures at a single magnesium alloy ingot casting machine. The measurements were conducted by URS Corporation (URS) at the Magnesium Refining Technologies (MagReTech) facility located in Bellevue, Ohio, throughout the week of 9 September 2007. Emissions were extracted and continuously analyzed in near real-time with Fourier Transform Infrared (FTIR) spectroscopy and quadrupole mass spectrometry Residual Gas Analysis (RGA). These analysis techniques enabled the simultaneous quantification of multiple concentrations in the cover gas environments at sub-ppmv-level sensitivities.

The three base gases evaluated in this study were sulfur hexafluoride (SF_6), pentafluoroethylhepafluoroisopropylketone (known by trade name Novec™ 612), and sulfur dioxide (SO_2). The cover gas mixtures are used to protect molten magnesium against surface burning during ingot casting. The primary objectives of this study are listed below.

- Characterize the cover gas destruction at this particular ingot casting tool. Destruction rates impact overall greenhouse gas (GHG) emissions. Destruction is defined as the percentage of base cover gas consumed by the process, whether by breakdown to a magnesium fluoride (MgF_2) film and subsequent chemical byproducts, or by direct conversion to byproducts from the thermal conditions and chemistries residing in the casting space environment.

- Characterize the ambient air dilution into the ingot casting and cooling environments. The hot zone and cold zone sections of the casting hood are not sealed, so air intrusion was expected to be significant. Ambient air dilution must be factored into the cover gas consumption considerations so that destruction rates can be properly filtered out from overall concentration reductions.

- Characterize the chemical byproducts produced for each cover gas mixture during ingot casting. The types and relative amounts of byproducts vary greatly depending on the base cover gas and the concentration at which it is used. The chemical byproducts produced also influence the global warming potential of the cover gas mixtures.

- Identify and detect low concentration occupational exposure emissions for each cover gas mixture. Using the most sensitive FTIR system available, monitor a worker area in close proximity to the hot zone for base cover gas and byproduct emissions.

The measurement schedule and test conditions are summarized in Table 1-1. Rather than being fixed, these conditions were what was encountered during facility operations at the time of

testing and resulted in a variety of cover gas mixture compositions over different alloy castings. The ingot casting machine parameters are summarized in Table 1-2.

Table 1-1.   Test Schedule and Process Conditions

Date (m/dd/yy)	Approx. Casting Time (Local Time)	Cover Gas Mixture Components[a]	Cover Gas Mixture Flows[b] (scfm)	Cover Gas Delivery Conc.[c] (ppmv)	Alloy Type
9/10/07	1730 – 1930	SF_6 / SO_2 / CDA / CO_2	0.08 / 0.02 / 6.8 / 7.4	10,675	AM50
9/11/07	1115 – 1345	SF_6 / SO_2 / CDA / CO_2	0.05 / 0.03 / 4.2 / 6.2	7,554	AZ91D
9/13/07	0915 – 1200	SF_6 / SO_2 / CDA / CO_2	0.07 / 0.04 / 5.5 / 8.7	8,463	AZ81
9/11/07	1500 – 1709	Novec-612 / CDA / CO_2	0.015 / 2 / 8	2,000	AZ91D
9/11/07	1709 – 1730	Novec-612 / CDA / CO_2	0.015 / 2 / 8	1,500	AZ91D
9/12/07	0915 – 1140	Novec-612 / CDA / CO_2	0.0125 / 2 / 8	1,102	AZ91D
9/12/07	1420 – 1620	Novec-612 / CDA / CO_2	0.015 / 2 / 8	1,663	AZ91D
9/13/07	1340 – 1540	SO_2 / CDA	0.10 / 4 / 6	10,000	AZ91D
9/14/07	0740 – 1000	SO_2 / CDA	0.12 / 4 / 6	12,000	AZ91D

[a] CDA = compressed dry air
[b] Approximate, estimated by reading flow rates on gas delivery manifold rotameters (uncalibrated)
[c] Measured directly at cover gas mix

Table 1-2. Magnesium Ingot Casting Machine Parameters

Parameter	Machine Specification[a]
Facility	MagReTech: Bellevue, OH
Ingot Casting Machine Type	Belt Caster
Ingot Weight (lbs)	25
Holding Furnace Capacity (lbs)	16,000 (per heat)
Alloy Type	All
Ingot Casting Rate (seconds/ingot)	12
Mg Pump Type	Centrifugal Pump
Metal Throughput (lbs/hr)	≈5,000
Heat Casting Duration (hours)	3-4
Ingot Mold Temperature (^{o}F)	120-200
Ingot Residence Time – Hot Zone (min)	0.5
Ingot Residence Time – Cold Zone (min)	2
Ingot Pour Control	Automatic Feed w/ Operator Override

[a]As provided by MagReTech

2. Methodology

All gas samples, whether from the casting hood environments or the worker exposure area, were extracted continuously from single points in space. The four sampling points located in the ingot casting area were 1) the upstream sampling point in the hot zone (denoted "hu"), 2) the downstream sampling point in the hot zone (denoted "hd"), 3) the upstream sampling point in the cold zone (denoted "cu"), and 4) the downstream sampling point in the cold zone (denoted "cd"). The sampling system is described in more detail in Section 2.1.2 and the schematic is presented as Figure 2-1.

This section of the report describes the field analytical methods used to probe the gas samples (FTIR and RGA are explained in Sections 2.1 and 2.2, respectively) and how ambient air dilution was determined within the casting hoods (Section 2.3).

2.1. Principles of FTIR Monitoring

Almost every chemical compound absorbs some amount of infrared (IR) light in a particular region of the mid-IR spectrum. These absorption properties can be used to identify and quantify chemical compounds in a complex mixture of gases. Beer's Law states that the magnitude of IR absorbance by a compound is directly proportional to the product of its concentration in the mixture and the sample cell optical path length. This product is otherwise known as the optical depth of a compound. The extractive FTIR instruments used by URS are able to achieve ppb detection levels because the optical path length within the measurement cell is magnified many times by reflecting the IR beam between a series of mirrors before it reaches the detector. The mirrors provide a fixed optical path length best suited to the gas mixture being sampled. For this study, optical path lengths of 10 m (for worker exposure monitoring), 5.11 m (for hot zone casting head space monitoring), and 20.1 m (for cold zone casting head space monitoring) were utilized.

2.1.1. The FTIR Spectrum Analysis Method

IR spectrum analysis matches the features of an observed spectrum to those of reference gases of known concentration. If more than one feature is present in the same region, then a linear combination of references is used to match the compound feature. The standards are scaled to match the observed band intensities in the sample. This scaling also matches the unknown concentrations. An IR spectrum can be collected and analyzed in approximately one second, but spectra are normally averaged over 1- to 5-min integration periods to produce adequate signal-to-noise limits and ppb detection levels.

The scaled references are added together to produce a composite that represents the best match with the sample. A classical least squares mathematical function is used to match the

absorption profiles of the standards with those of the observed spectrum in specified spectral analysis regions. The compounds of interest and the compounds expected to cause spectral interference are included in the analysis region.

The spectrum analysis methods used for this study were developed by selecting the spectral regions that were least affected by primary IR absorbers (in this case, H_2O and CO_2) while also producing the best detection limits possible for cover gas compounds and potential byproducts. Target compounds were determined prior to sampling based on previous tests of similar cover gas composition. The analysis methods were iteratively refined by analyzing representative sets of IR spectra while varying quantitative analysis parameters until optimum methods were established. Methods are optimum when the 95 percent confidence levels (the errors indicating goodness-of-fit) and the absolute bias of all analytes are minimized. Table 2-1 lists the calibration reference set ranges, as they pertain to their respective cover gas mixture, for all the compounds monitored throughout the MagReTech study. This represents a complete list of potential and existing contaminants, though not all of these contaminants were observed during the study, as later reported in Section 3.

Table 2-1.   Parameters for Major Contaminants and Spectroscopic Interferants

Chemical Formula	Compound	SF_6 (ppmv-meters)	Novec™ 612 (ppmv-meters)	SO_2 (ppmv-meters)
H_2O	Water	2.89 - 22.3*	2.89 - 22.3*	2.89 - 22.3*
CO_2	Carbon Dioxide	70 - 2,110	137 - 510*	70 - 2,110
SF_6	Sulfur Hexafluoride	58 - 92,701	56 - 280	56 - 280
$C_3F_7C(O)C_2F_5$	Novec™ 612	n/a	99 - 991	n/a
SO_2	Sulfur Dioxide	518 - 10,415	n/a	518 - 35,770
CO	Carbon Monoxide	26 - 20,358	784 - 20,358	26 - 3,863
HF	Hydrofluoric Acid	1 - 2,000	1 - 2,000	1 - 2,000
COF_2	Carbonyl Fluoride	50 - 5,000	50 - 5,000	n/a
C_2H_2	Acetylene	111 - 5,550	111 - 5,550	n/a
C_2H_4	Ethylene	86 - 2,576	86 - 2,576	86 - 2,576
C_2F_6	Hexafluoroethane	448 - 1,119	448 - 1,119	n/a
CF_4	Carbon Tetrafluoride	5.6 - 1,120	5.6 - 1,120	n/a
CHF_3	Trifluoromethane	112 - 560	112 - 560	n/a
CH_3F	Methyl Fluoride	177 - 1,182	177 - 1,182	n/a
CH_4	Methane	87 - 21,119	87 - 21,119	87 - 21,119
CH_2O	Formaldehyde	92 - 1,838	92 - 1,838	92 - 1,838
CH_2O_2	Formic Acid	76	76	76
NO	Nitric Oxide	53 - 2,043	53 - 2,043	53 - 2,043
N_2O	Nitrous Oxide	102 - 1,019	102 - 1,019	102 - 1,019
NO_2	Nitrogen Dioxide	34 - 1,544	34 - 1,543	34 - 1,543
H_2SO_4	Sulfuric Acid	n/a	n/a	164
SO_3	Sulfur Trioxide	n/a	n/a	1,400

*Expressed in percent-meters since high concentration references were required.

Sensitivities associated with the optimized analysis methods are highly field dependent because they are subject to overall moisture content (which affects the IR detector signal-to-noise ratio) and to sample matrix content (which adds interferences to quantification regions). Therefore, detection limits are discussed in Section 3 and Section 4 as they relate to the field measurements of low concentration byproducts and worker exposure compounds.

2.1.2. The Extractive FTIR Systems

Three extractive FTIR systems were used in this study. MKS (On-Line) FTIR spectrometers were used to analyze the casting hood environments, while a Thermo-Nicolet spectrometer was used to monitor the worker exposure location. Stainless steel sample probes (¼-inch out diameter (OD)) were used to extract gas samples via venturi pumps connected to the exhaust of the short path (5.11 m) sample cell for the hot zone and of the long path (20.1 m) sample cell for the cold zone. A long perfluoroalkoxy (PFA) Teflon line (¼-inch OD) acted as the sample probe at the worker exposure location. Flows on the order of 5 lpm were maintained through each extraction system. The sample flow temperatures were maintained at 150 ^{o}C at the casting hood locations and at room temperature (~30 ^{o}C) at the worker exposure location. The casting hood FTIR systems maintained elevated temperatures for their sample cells and extraction lines to preclude condensation loss and acid mist formation. There were two sampling port locations for both the hot zone and cold zone casting hood areas – an upstream location closest to the casting pours and a downstream location farthest from the casting pours. The stainless steel probes within each hood area were moved from upstream locations to downstream locations for periods of continuous sampling at each location. The probes extended about 6 inches into the casting hood. Approximate dimensions and configurations are indicated in the sampling schematic (Figure 2-1).

Inside each FTIR cell, a set of optically matched gold-plated mirrors reflected an IR beam through the sample gas multiple times. As the beam passes through the sample, the molecules in the sample absorb some of its energy. After exiting the cell, the IR beam was directed to a liquid-nitrogen cooled-mercury/cadmium/telluride (MCT) detector, which is a photoconductive device that produces an electrical voltage proportional to the amount of IR energy that strikes it. The magnitude of IR absorbance at particular frequencies is a measure of the concentrations of chemical compounds. The cell path length is the total distance traveled by the IR beam inside the cell and is an important variable used to determine sample concentrations. For this project, cell path lengths were fixed at 20.1 m for the casting hood cold zone FTIR, 5.1 m for the hot zone FTIR, and 10 m for the worker exposure monitoring system. Interferometer resolutions were set to 0.5 cm^{-1} and signal averaging was performed over two-min periods.

(not to scale)
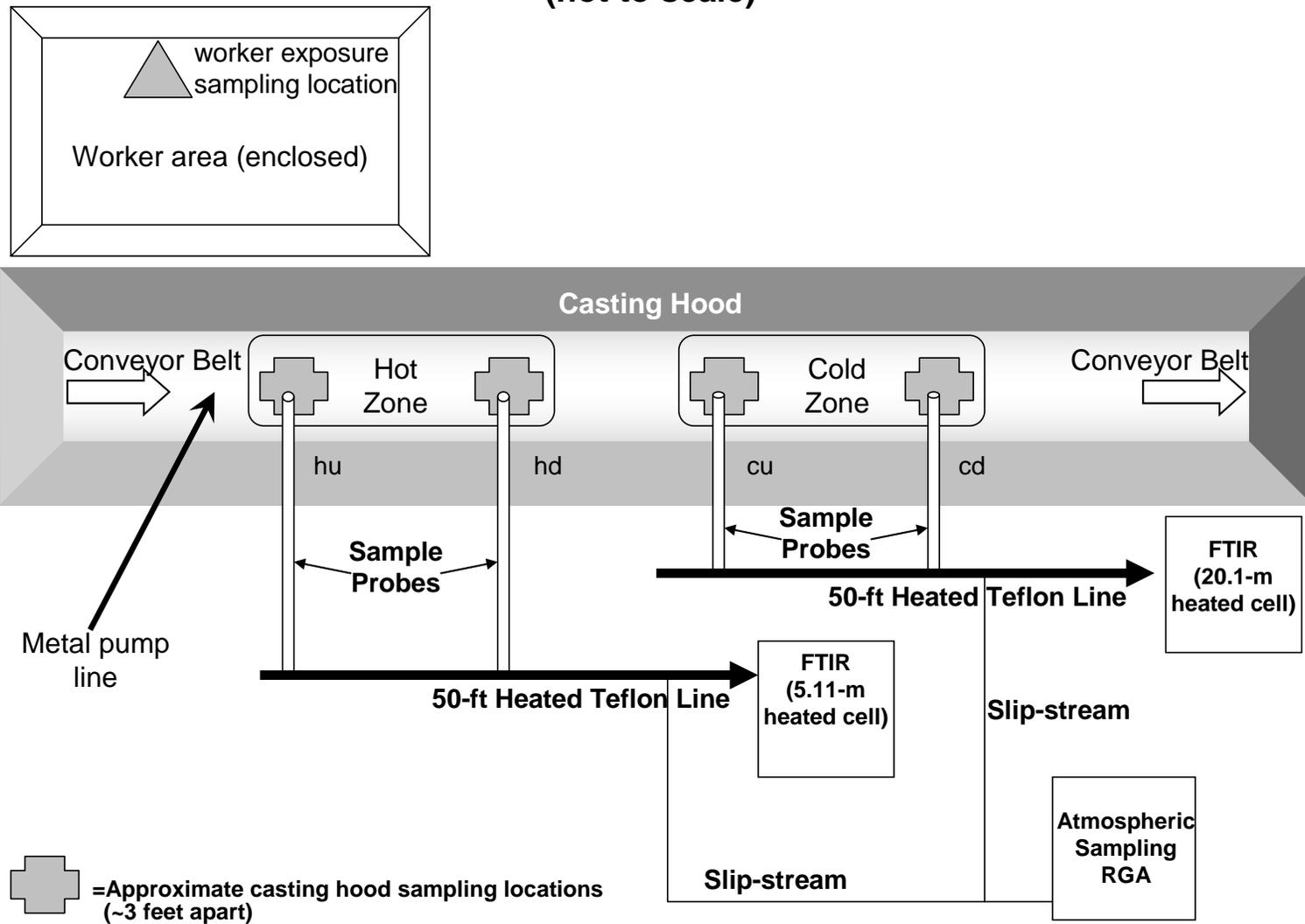
Figure 2-1.   Casting Hood and Sampling System Schematic

2.2. Principles of RGA Monitoring

A mass spectrum is obtained by converting components of a sample into rapidly moving gaseous ions and resolving them on the basis of their mass-to-charge ratios. The principles of mass spectrometry are straightforward; a block diagram showing the major components of the URS-built RGA is displayed in Figure 2-2.
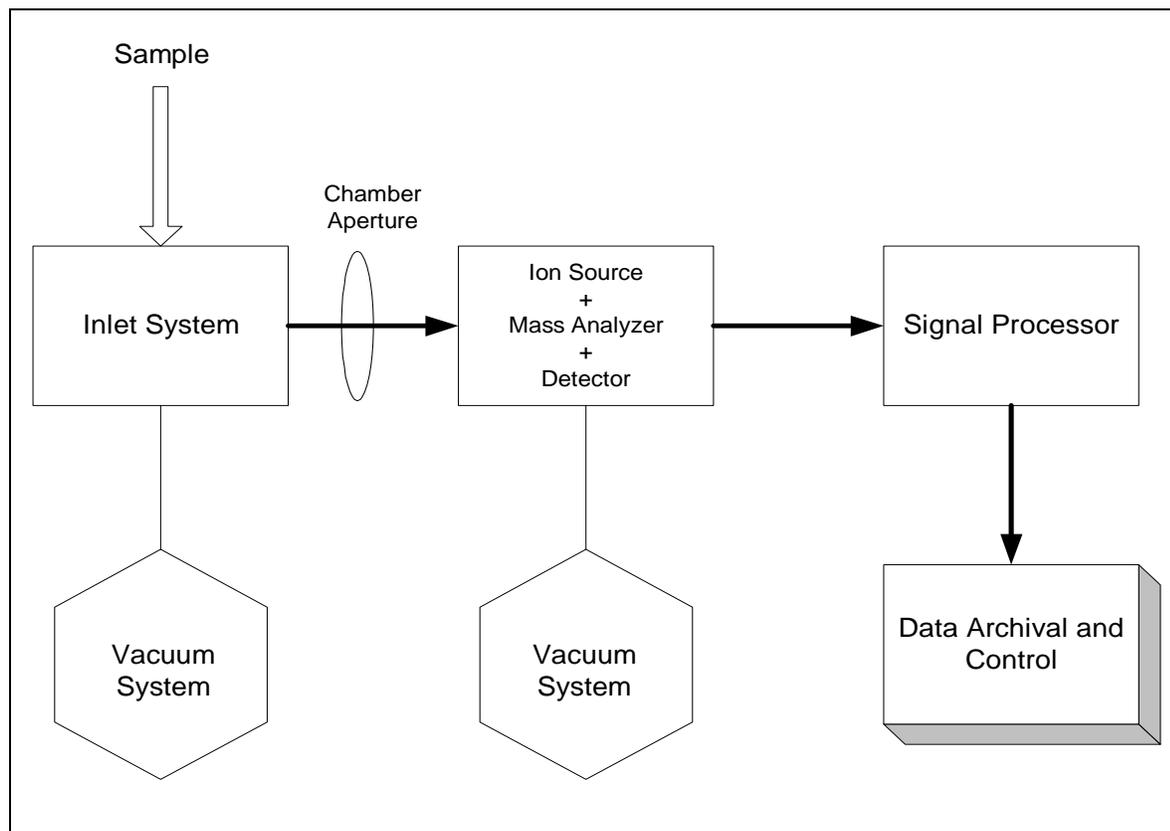
Figure 2-2.   RGA Component Block Diagram

Descriptions of these components are included in Section 2.2.2. As molecules from the sample are ionized in the analyzer chamber, the detector registers a response for a given mass-to-charge (m/e) ratio at an intensity proportional to the absolute molecule count. The following section reports the desired m/e ratios for argon and krypton, which were monitored during dilution measurements.

2.2.1. The RGA Spectrum Analysis Method

Since the RGA quadrupole mass analyzer breaks down molecules (or, in this case, the natural atomic species argon or krypton) into fragments of varying m/e ratios, the specific m/e

for each compound of interest that leads to the greatest response at the detector was targeted. Table 2-2 lists the relative isotopic abundances in nature for argon and krypton.

Table 2-2.   Relative Isotopic Abundances for Argon and Krypton

Isotope	Accurate Mass (m/e, unitless)	Abundance (percent)
36-Ar	35.9675456	0.3380
38-Ar	37.9627322	0.0630
40-Ar	39.9623831	100.0000
78-Kr	77.9203970	0.6140
80-Kr	79.9163750	3.9474
82-Kr	81.9134830	20.3509
83-Kr	82.9141340	20.1754
84-Kr	83.9115060	100.0000
86-Kr	85.9106140	30.3509

According to the information in Table 2-2, the derived m/e value for the "parent" argon ion is 40 and for krypton is 84. As a result, rather than scanning across each m/e channel within its measurement range of 2 to 100 amu, the analyzer was focused directly to either m/e = 40 or m/e = 84. A few other m/e values were scanned during monitoring periods for diagnostic purposes, including parent ions for nitrogen, oxygen, water, and carbon dioxide. In order to enable measurements of dilution percentage, the RGA detector response is calibrated periodically by relating known argon and krypton concentrations to the detector signal. RGA calibrations are reported in Appendix A and the dilution determinations are reported in Section 4.

2.2.2. The Extractive RGA System

Traditionally, mass spectrometers are used in a vacuum. Coupled with the development of atmospheric samplers and closed ion sources, recent advancements of this technology have enabled atmospheric sampling. The "high pressure" URS-built RGA is smaller, more robust, and much more portable than its laboratory predecessors. Gas samples were brought to the mass analyzer vacuum chamber as slip-streams from the FTIR sample inlets via a venturi pump. The pump provided the sample matrix at less-than-atmospheric (~500 torr) pressures and with small residence times within the sample line tubing. The venturi pump extraction region, which is basically the inlet of the pump, was interfaced to the RGA sample chamber with a small orifice valve that was manually tuned to maintain a reasonable leak rate into the sample chamber. This orifice valve was separated from the mass analyzer chamber by a small diameter ($< 100 \ \mu m$) aperture. The inlet system was set to maintain a sample pressure of $\sim 5 \times 10^{-4}$ torr, which was an increase of two orders of magnitude over the mass analyzer chamber background pressure and which was maintained by turbomolecular pump. Given an argon or krypton tracer concentration

of approximately 1 percent (10,000 ppmv), a detection sensitivity of approximately 100 ppmv was achieved. Such a detection sensitivity enabled the accurate measurement of dilution percentage values up to 99 percent (1-[100 ppmv / 10,000 ppmv] * 100).

The RGA detection system housed in the main (mass analyzer) chamber was a Micropole™ mass analyzer manufactured by Horiba. It consisted of an integrated package that operated a tungsten filament (the ionizer) coupled to a series of focusing lenses and a miniature array of quadrupoles (the mass analyzer) that allowed the ions to strike a Faraday Cup (the detector). The mass range for this analyzer was 2 to 100 amu with a resolution of 1 amu. A RS232 digital interface to a laptop and appropriate software allowed continuous operation and data archival.

2.3. Ambient Air Dilution Considerations

Though the ingot casting machine hot and cold zones were somewhat contained in a hooded enclosure, they were not completely sealed. A significant amount of ambient air dilution was anticipated and must be considered when computing destruction rates based on concentration measurements. As a result, the ambient air dilution within the casting hood was experimentally determined using three distinct approaches.

1) Ambient argon intrusion: This was anticipated to provide the most direct and continuous measurement approach because the concentration of argon was tracked in real time via RGA at the same extractive sample locations as the FTIR systems. Ambient levels of argon were assumed to be on the order of 1 percent (10,000 ppmv) and were factored into the dilution calculations when known flow rates of compressed dry air (CDA) from the direct cover gas mixture were considered supplemental to air dilution. Therefore, given the field RGA sensitivity for argon on the order of 100 ppmv, dilution rates up to 99 percent could be tracked. With only one RGA system available for sampling, the hot casting zone was monitored during the first half of each cover gas testing period and the cold casting zone was monitored during the second half of the period.

2) Krypton tracer: A krypton tracer study was intended to further support the direct argon intrusion measurements. An added benefit of this part of the study was that krypton background concentrations and cover gas mixture contributions were negligible, which minimizes dilution rate bias. One point of concern in this analysis was the possibility of krypton interacting with free fluorine in the thermal plasma at the magnesium melt surface. The heavy noble gas xenon will readily form complexes with fluorine and oxygen, while the reactivity of krypton is less known but is expected to be weaker than with xenon.

3) Cover gas measurements during non-casting periods: Because casting operations at MagReTech were constant while the cover gas was being applied, measurements taken from the casting hood during normal testing conditions (a moving ingot mold conveyer belt with metal present) could be compared to a situation with a moving belt but no metal present. Since no magnesium was present in the casting hood zones to react with or degrade the cover gas, any reduction in the concentration of the cover gas constituents would be solely attributable to ambient air dilution. This test was run once for each cover gas system examined. A potential anticipated drawback to this procedure was that the ambient air/cover gas dilution dynamics may be different in a casting hood without molten magnesium and its resulting convective effects, though ingot molds are pre-heated. The dilution estimates determined through this approach were then used to determine cover gas destruction.

Injecting argon tracer gas directly into the cover gas mixture manifold at concentrations much greater than ambient levels would further support the results obtained from the ambient argon intrusion monitoring. High tracer concentrations are needed to overcome not only the native amounts of argon present due to significant ambient air dilution but also the argon already present in the CDA. High concentrations of inert tracer gas would potentially have an adverse impact on the cover gas mixture needed for processing ingots by displacing the active cover gas constituents. Therefore, only the three approaches described above were carried out, and the results of these approaches are reported in Section 4.

3. Monitoring Results

3.1. Casting Hood Monitoring

Each cover gas mixture has the potential to generate a variety of chemical byproducts that are due to local thermal plasma effects near the ingot melt surfaces in conjunction with significant amounts of ambient moisture within the casting hood environment. The amount of air dilution was expected to impact the type and relative amounts of these byproducts, but the extent of this impact is not completely understood. For example, air dilution provides a source of hydrogen as a chemical pathway so that all fluorinated cover gas mixtures (SF_6/SO_2 and Novec™ 612) were expected to produce a hydrogen fluoride (HF) byproduct. Also, the thermal plasmas within the local volumes around each ingot mold were expected to break down the base cover gas mixture components into reactive atomic and free radical species. These species would then recombine into other byproducts that were mostly fluorinated. This would be especially true for Novec™ 612 mixtures, as perfluorocarbons (PFCs) have previously been observed during tests conducted on magnesium die casting holding furnaces.[5]

However, for this project, the expected byproducts normally produced at low ppmv levels were not analytically detected because of the small surface areas of the magnesium melts and the high degree of dilution in the ingot casting hood. Table 3-1 summarizes the cover gas, ambient air, and combustion-type compounds and the expected destruction byproducts for the SF_6/SO_2 cover gas runs. The minimum detection limits (MDLs) for the anticipated byproducts are also reported. These MDLs were considered to be field-representative by taking three times the standard deviation of the quantitative analysis values for each compound that were scattered about zero. The sample spectra data sets were validated by confirming that they contained all the primary infrared absorption interferences (for H_2O, CO_2, base cover gas compounds, etc.) but none of the byproducts listed as not detected (ND) in the tables below. Tables 3-2 and 3-3 summarize the observable compounds for the Novec™ 612 cover gas runs. In tests 5hd and 6hd, CHF_3 was measured at extremely low levels, averaging at or below the MDL. Table 3-4 summarizes the observables for the SO_2 cover gas mixture. Sulfuric acid (H_2SO_4) was anticipated but not detected throughout both sampling periods.

Special attention was paid to perfluoroisobutylene (PFIB) as one potential byproduct of the Novec™ 612 cover gas mixture. It was important to monitor PFIB from an occupational exposure standpoint because it is has extremely low exposure limits. A suitable FTIR spectral reference was unattainable, and the URS laboratory was not able to generate a reference because PFIB is a controlled substance. However, a mass spectrum of this gas has been published and was referenced on-site against a continuous two-hour block of full-spectral RGA scans taken during the Novec™ 612 testing. The appearance of RGA peaks at m/e = 69, 31, and 93 at

---

[5] US EPA. *Characterization of Emissions and Occupational Exposure Associated with Five Cover Gas Technologies for Magnesium Die Casting*, 2007

relative abundances of 100 percent, 60 percent, and 30 percent, respectively, would have been an indicator of the presence PFIBs. However, PFIB was not detected during this study because signals at m/e = 69 were never observed to be above noise levels. The estimated detection limit for partial pressures at m/e = 69 was on the order of 10 ppmv.

Table 3-1. Data Summary for SF_6 / SO_2 Cover Gas Mixture

Date	Test Location		SF_6 (ppmv)	SO_2 (ppmv)	H_2O (%)	CO_2 (%)	CO (ppmv)	CH_4 (ppmv)	HF (ppmv)	COS (ppmv)	CS_2 (ppmv)	H_2S (ppmv)	H_2SO_4 (ppmv)
9/10/07	Direct		10,675	4,039									
	1hu	Min	1,332	502	1.04	6.21	0.41	2.54	0.05	ND	ND	ND	ND
		Max	1,478	547	1.25	6.56	1.95	10.0	0.17	ND	ND	ND	ND
		Avg	1,407	530	1.09	6.42	0.83	3.79	0.09	ND	ND	ND	ND
		MDL								0.01	0.44	8.46	0.34
	1cu	Min	507	210	0.94	2.36	0.50	2.40	0.26	ND	ND	ND	ND
		Max	646	265	1.07	2.87	2.14	9.63	0.30	ND	ND	ND	ND
		Avg	572	233	0.97	2.67	0.96	3.81	0.28	ND	ND	ND	ND
		MDL								0.01	1.17	22.5	0.34
9/11/07	Direct		7,554	8,249									
	2hu	Min	1,016	605	1.18	6.18	0.20	2.19	0.02	ND	ND	ND	ND
		Max	1,418	1,127	1.49	7.52	5.88	3.61	0.07	ND	ND	ND	ND
		Avg	1,251	724	1.34	7.12	0.56	2.66	0.03	ND	ND	ND	ND
		MDL								0.03	0.61	15.5	0.64
	2cu	Min	375	199	0.79	1.85	0.17	2.10	0.09	ND	ND	ND	ND
		Max	537	411	0.96	2.57	4.04	3.41	0.15	ND	ND	ND	ND
		Avg	456	232	0.88	2.11	0.48	2.61	0.11	ND	ND	ND	ND
		MDL								0.03	2.11	28.8	0.49
9/13/07	Direct		8,463	6,682									
	3hu	Min	648	449	1.07	3.86	0.43	2.54	0.07	ND	ND	ND	ND
		Max	1,651	1016	1.54	8.32	64.6	371	0.11	ND	ND	ND	ND
		Avg	1,232	843	1.27	6.81	10.1	56.1	0.09	ND	ND	ND	ND
		MDL								0.03	0.75	19.2	1.08
	3cu	Min	442	298	0.58	1.72	0.34	1.91	0.08	ND	ND	ND	ND
		Max	865	557	1.03	3.08	138	354	0.26	ND	ND	ND	ND
		Avg	639	446	0.75	2.64	32.9	82.8	0.17	ND	ND	ND	ND
		MDL								0.06	0.76	37.2	1.06
	3hd	Min	283	143	1.11	242	0.27	2.14	0.07	ND	ND	ND	ND
		Max	565	322	1.48	3.59	1.64	9.87	0.11	ND	ND	ND	ND
		Avg	424	216	1.28	2.91	0.62	3.24	0.09	ND	ND	ND	ND
		MDL								0.01	1.00	18.6	2.92
	3cd	Min	236	126	0.73	1.53	0.33	1.49	0.18	ND	ND	ND	ND
		Max	499	396	0.85	2.58	2.21	4.42	0.37	ND	ND	ND	ND
		Avg	333	187	0.78	1.92	0.72	2.68	0.26	ND	ND	ND	ND
		MDL								0.04	0.34	46.9	1.30

MDL is reported if the compound was not detected (ND).

Table 3-2. Data Summary for MTG-Shield™ using Novec™ 612

Date	Test Location		Novec™ 612 (ppmv)	H_2O (%)	CO_2 (%)	CO (ppmv)	CH_4 (ppmv)	HF (ppmv)	SF_6 (ppmv)	CHF_3 (ppmv)	CF_4 (ppmv)	C_2F_6 (ppmv)	C_3F_8 (ppmv)	COF_2 (ppmv)	CH_2O_2 (ppmv)	H_2CO (ppmv)
9/11/07	Direct		2,000													
	4hu	Min	196	1.00	6.82	1.09	2.84	0.11	0.49	ND	ND	ND	ND	ND	ND	ND
		Max	247	1.28	8.78	2.44	4.55	0.24	0.77	ND	ND	ND	ND	ND	ND	ND
		Avg	219	1.15	7.81	1.94	3.74	0.17	0.64	ND	ND	ND	ND	ND	ND	ND
		MDL								0.16	1.34	0.67	0.24	0.18	0.69	0.05
	4cu	Min	70.4	0.76	2.21	0.87	4.39	0.22	0.65	ND	ND	ND	ND	ND	ND	ND
		Max	86.4	0.91	2.86	1.73	5.99	0.35	0.96	ND	ND	ND	ND	ND	ND	ND
		Avg	76.9	0.84	2.59	1.40	5.17	0.31	0.79	ND	ND	ND	ND	ND	ND	ND
		MDL								0.27	0.63	0.06	0.08	0.16	0.21	0.10
	Direct		1,500													
	5hd	Min	43.7	1.02	2.24	0.81	3.27	0.12	0.57	ND	ND	ND	ND	ND	ND	ND
		Max	49.4	1.14	2.50	1.12	4.09	0.17	0.73	0.30	ND	ND	ND	ND	ND	ND
		Avg	47.0	1.07	2.40	0.95	3.69	0.15	0.64	0.15	ND	ND	ND	ND	ND	ND
		MDL								0.15	2.05	0.17	0.25	0.18	0.45	0.06
	5cd	Min	26.3	0.77	1.30	0.59	4.71	0.19	0.79	ND	ND	ND	ND	ND	ND	ND
		Max	27.9	0.84	1.34	0.84	5.96	0.23	0.91	ND	ND	ND	ND	ND	ND	ND
		Avg	27.0	0.80	1.31	0.72	5.31	0.22	0.86	ND	ND	ND	ND	ND	ND	ND
		MDL								0.37	1.36	0.12	0.09	0.33	0.15	0.17

MDL is reported if the compound was not detected (ND).

Table 3-3. Data Summary for MTG-Shield™ using Novec™ 612

Date	Test Location		Novec™ 612 (ppmv)	H_2O (%)	CO_2 (%)	CO (ppmv)	CH_4 (ppmv)	HF (ppmv)	SF_6 (ppmv)	CHF_3 (ppmv)	CF_4 (ppmv)	C_2F_6 (ppmv)	C_3F_8 (ppmv)	COF_2 (ppmv)	CH_2O_2 (ppmv)	H_2CO (ppmv)
9/12/07	Direct		1,102													
	6hu	Min	77.5	0.96	4.79	0.45	1.77	0.05	0.07	ND	ND	ND	ND	ND	ND	ND
		Max	112	1.28	7.16	3.35	2.86	0.16	0.22	ND	ND	ND	ND	ND	ND	ND
		Avg	95.6	1.12	6.66	1.66	2.12	0.09	0.11	ND	ND	ND	ND	ND	ND	ND
		MDL								0.09	1.58	0.41	0.29	0.16	0.76	0.05
	6cu	Min	137	2.46	8.33	0.72	3.56	0.35	0.28	ND	ND	ND	ND	ND	ND	ND
		Max	223	2.97	11.0	9.78	10.7	0.82	1.09	ND	ND	ND	ND	ND	ND	ND
		Avg	161	2.67	9.17	2.44	7.45	0.61	0.50	ND	ND	ND	ND	ND	ND	ND
		MDL								0.90	5.21	0.81	0.26	0.53	1.17	0.61
	6hd	Min	34.9	1.15	2.99	0.61	2.09	0.14	0.08	ND	ND	ND	ND	ND	ND	ND
		Max	41.3	1.58	3.61	105	719	0.18	0.32	0.30	ND	ND	ND	ND	ND	ND
		Avg	37.5	1.30	3.22	10.7	71.1	0.17	0.16	0.15	ND	ND	ND	ND	ND	ND
		MDL								0.22	1.48	1.10	0.64	0.17	1.12	0.05
	6cd	Min	52.1	2.60	4.79	0.87	10.2	0.73	0.63	ND	ND	ND	ND	ND	ND	ND
		Max	84.1	3.63	5.24	436.5	1558	1.29	1.75	ND	ND	ND	ND	ND	ND	ND
		Avg	73.8	2.86	4.99	36.8	139	0.97	0.99	ND	ND	ND	ND	ND	ND	ND
		MDL								1.92	7.95	0.39	0.22	0.53	0.54	0.66
9/12/07	Direct		1,663													
	7hu	Min	85.7	0.98	3.93	0.26	1.32	0.12	0.04	ND	ND	ND	ND	ND	ND	ND
		Max	158	1.21	6.35	0.93	2.32	0.38	0.13	ND	ND	ND	ND	ND	ND	ND
		Avg	131	1.10	5.25	0.52	1.82	0.26	0.08	ND	ND	ND	ND	ND	ND	ND
		MDL								0.22	1.48	1.10	0.64	0.17	1.12	0.05
	7cu	Min	203	2.60	7.30	0.62	4.57	0.85	0.09	ND	ND	ND	ND	ND	ND	ND
		Max	260	3.31	9.47	2.57	9.85	1.47	0.52	ND	ND	ND	ND	ND	ND	ND
		Avg	228	2.91	8.44	1.20	6.93	1.16	0.28	ND	ND	ND	ND	ND	ND	ND
		MDL								0.60	3.10	0.40	0.19	0.28	0.71	0.20

MDL is reported if the compound was not detected (ND).

Table 3-4.   Data Summary for SO_2 Cover Gas Mixture

Date	Location		SO_2 (ppmv)	H_2O (%)	CO_2 (%)	CO (ppmv)	CH_4 (ppmv)	COS (ppmv)	CS_2 (ppmv)	H_2S (ppmv)	H_2SO_4 (ppmv)
9/13/07	Direct		10,000								
	8hd	Min	221	0.89	2.20	0.14	3.32	ND	ND	ND	ND
		Max	295	1.13	2.40	0.66	3.99	ND	ND	ND	ND
		Avg	277	0.95	2.27	0.28	3.62	ND	ND	ND	ND
		MDL						0.004	3.54	24.6	0.05
	8cd	Min	103	0.75	0.94	0.16	2.82	ND	ND	ND	ND
		Max	142	0.84	1.13	0.43	4.01	ND	ND	ND	ND
		Avg	128	0.80	0.99	0.29	3.18	ND	ND	ND	ND
		MDL						0.02	2.34	33.4	0.02
9/14/07	Direct		12,000								
	9hu	Min	539	1.08	0.04	0.23	2.67	ND	ND	ND	ND
		Max	1,077	1.34	7.21	1.95	4.03	ND	ND	ND	ND
		Avg	946	1.22	1.06	0.53	3.40	ND	ND	ND	ND
		MDL						0.01	2.09	18.5	0.07
	9cu	Min	263	0.67	0.04	0.28	2.94	ND	ND	ND	ND
		Max	320	0.82	0.04	4.30	4.09	ND	ND	ND	ND
		Avg	296	0.75	0.04	0.88	3.42	ND	ND	ND	ND
		MDL						0.03	1.20	19.3	0.03

MDL is reported if the compound was not detected (ND).

3.2. Worker Exposure Monitoring

The cover gases evaluated in this study can produce byproducts that may be of concern from an occupational exposure standpoint. Therefore, a third extractive FTIR system was used to monitor the ambient air in the casting machine operator room (see Figure 2-1) for any potential occupational exposure hazards associated with the usage of each cover gas. For example, SO_2 and HF have very low eight-hour time-weighted average exposure limits of 2 and 3 ppmv, respectively.[6] The breathing zone located near the worker responsible for controlling ingot pours and skimming ingot surfaces was continuously monitored during the testing. Table 3-5 summarizes the concentrations observed, as well as the pertinent MDLs for the compounds not detected, for those species present in the casting hood at the highest concentrations – namely the primary cover gas compounds and the most significant byproduct (HF). Only SF_6 was observed, and only during its usage as a cover gas. The spectra were surveyed for the appearance of features attributable to compounds outside of those listed in Table 2-1 but none were observed besides expected ambient air constituents.

Table 3-5.   Worker Exposure Monitoring

Date (m/dd/yy)	Approx. Casting Time (Local Time)	Cover Gas Mixture Components	Average SF_6 (ppmv)	Average SO_2 (ppmv)	Average Novec™ 612 (ppmv)	Average HF (ppmv)
9/10/07	1730 - 1930	SF_6/ SO_2/ CDA / CO_2	0.22	< 0.5	n/a	< 0.1
9/11/07	1115 - 1345	SF_6/ SO_2/ CDA / CO_2	0.19	< 0.5	n/a	< 0.1
9/13/07	0915 - 1200	SF_6/ SO_2/ CDA / CO_2	0.57	< 0.5	n/a	< 0.1
9/11/07	1500 - 1709	Novec™ 612 / CDA / CO_2	n/a	n/a	< 2.0	< 0.1
9/11/07	1710 - 1730	Novec™ 612 / CDA / CO_2	n/a	n/a	< 2.0	< 0.1
9/12/07	0915 - 1140	Novec™ 612 / CDA / CO_2	n/a	n/a	< 2.0	< 0.1
9/12/07	1420 - 1620	Novec™ 612 / CDA / CO_2	n/a	n/a	< 2.0	< 0.1
9/13/07	1340 - 1540	SO_2/ CDA	n/a	< 0.5	n/a	< 0.1
9/14/07	0740 - 1000	SO_2/ CDA	n/a	< 0.5	n/a	< 0.1

Compounds listed with values as < X were not observed; their detection limits are reported as the value X.

n/a – not applicable

---

[6] OSHA Permissible Exposure Limits (PELs), http://www.osha.gov

4. Cover Gas Destruction

Throughout each casting run listed in Table 1-1, the primary cover gas components and byproducts were quantified simultaneously at both the casting hood hot zone and the cold zone (see Figure 2-1). Roughly half of each monitoring period was spent sampling the upstream ports; the other half was spent at the downstream ports. On some occasions, it was possible to monitor at these sampling ports while the ingot casting conveyor was moving and still heated but with no magnesium being poured: this was known as a "noncasting condition". In addition, on some occasions it was possible to sample the cover gas composition at the outlet of the gas blending manifold before injection into the casting hood. This was known as a "direct" cover gas mixture measurement. Average concentrations over the sampling periods were then used to calculate cover gas destruction percentages via the following approach:

Consider the injection cover gas concentration (after factoring in ambient air dilution) versus the cover gas concentrations at the sampled locations. Calculate the destruction factor (DF) as a percentage using

$$DF = 100 \times \left[1 - \frac{\text{sample cover gas conc. (ppm)}}{\text{direct cover gas conc. (ppm)}} \times \frac{1}{\left(1 - \dfrac{DP}{100}\right)} \right]$$

where DP is the dilution percentage, which is determined experimentally by krypton tracer or argon intrusion and casting vs. noncasting monitoring, as reported in Section 4.1.

The concentration and DF results for each cover gas mixture are reported in section 4.2.

4.1. Determining Dilution

Figures 4-1, Figure 4-2, Figure 4-3 plot the RGA-measured concentrations for argon and krypton as the detector responses at m/e = 40 and m/e = 84 were isolated for each mass spectrum and converted to concentrations via the appropriate calibration curve. Each graph corresponds to a period of time when a krypton tracer was injected into the cover gas blending manifold with a flow producing concentrations on the order of 0.5 – 1 percent. Therefore, dilution percentages were determined redundantly by simultaneous measurement of both direct argon intrusion and krypton tracer. Notated on each graph is when the monitoring occurred at a specific sampling location (upstream hot zone, downstream hot zone, upstream cold zone, downstream cold zone, and cover gas direct).
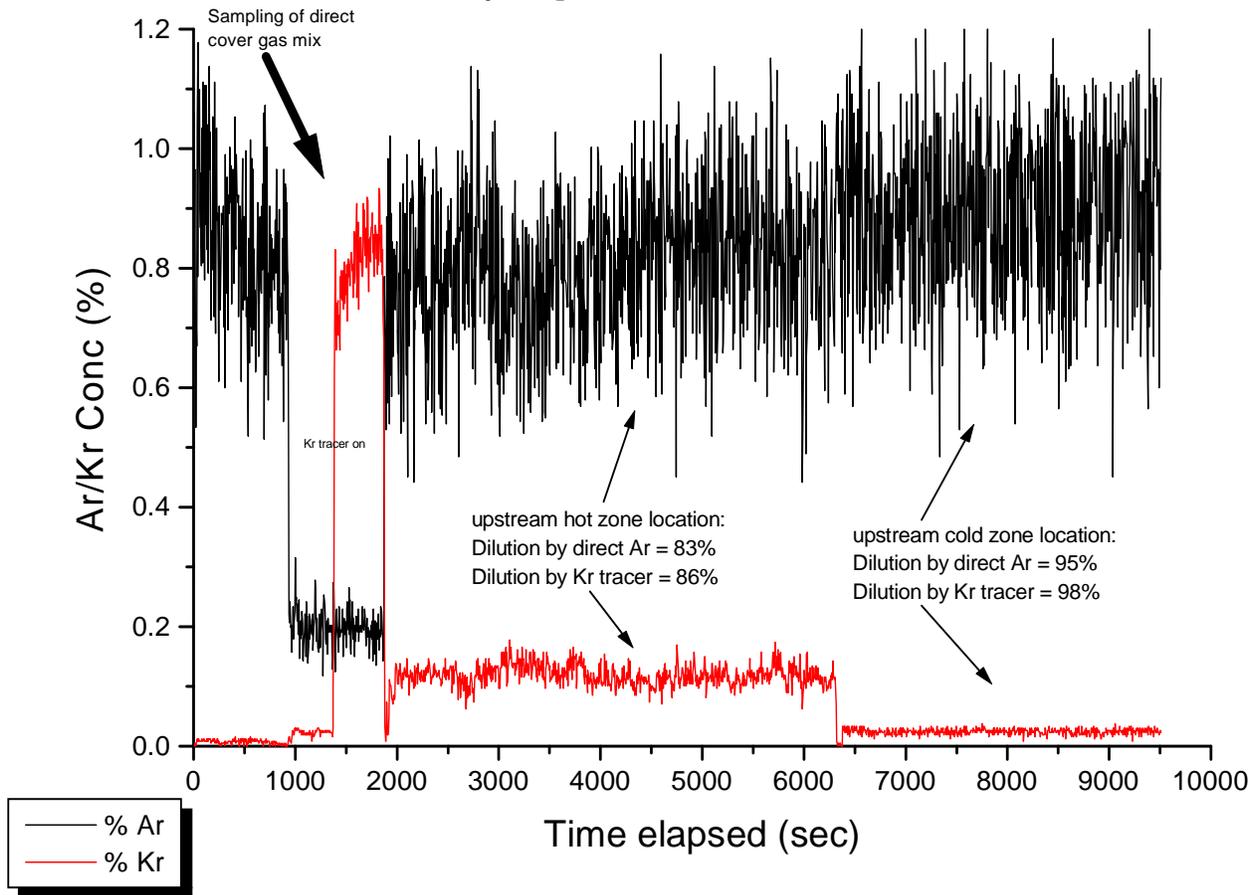
Figure 4-1.   RGA Dilution Measurements, 11 September 2007

RGA Dilution Determination: Kr Tracer and Direct Ar Monitoring
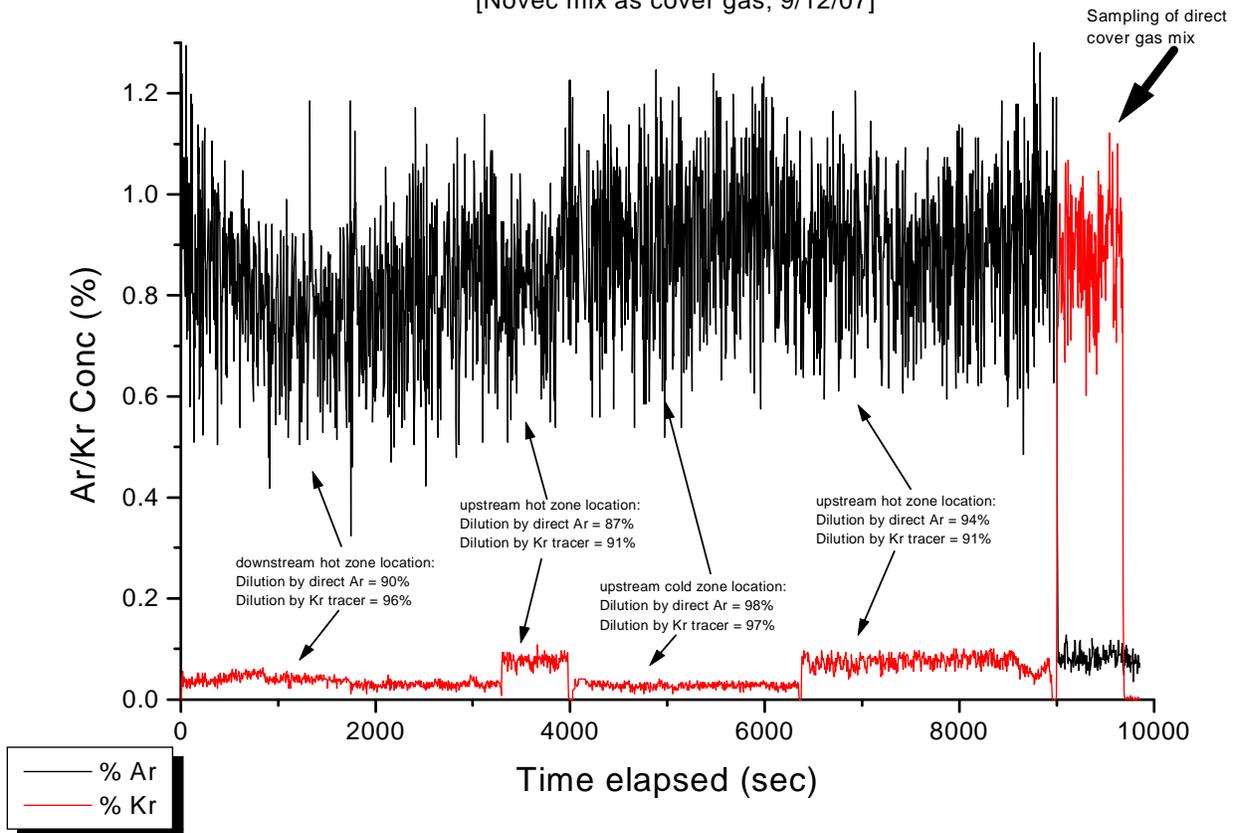### [Novec mix as cover gas; 9/12/07]

Sampling of direct cover gas mix

downstream hot zone location:
Dilution by direct Ar = 90%
Dilution by Kr tracer = 96%

upstream hot zone location:
Dilution by direct Ar = 87%
Dilution by Kr tracer = 91%

upstream cold zone location:
Dilution by direct Ar = 98%
Dilution by Kr tracer = 97%

upstream hot zone location:
Dilution by direct Ar = 94%
Dilution by Kr tracer = 91%

% Ar
% Kr

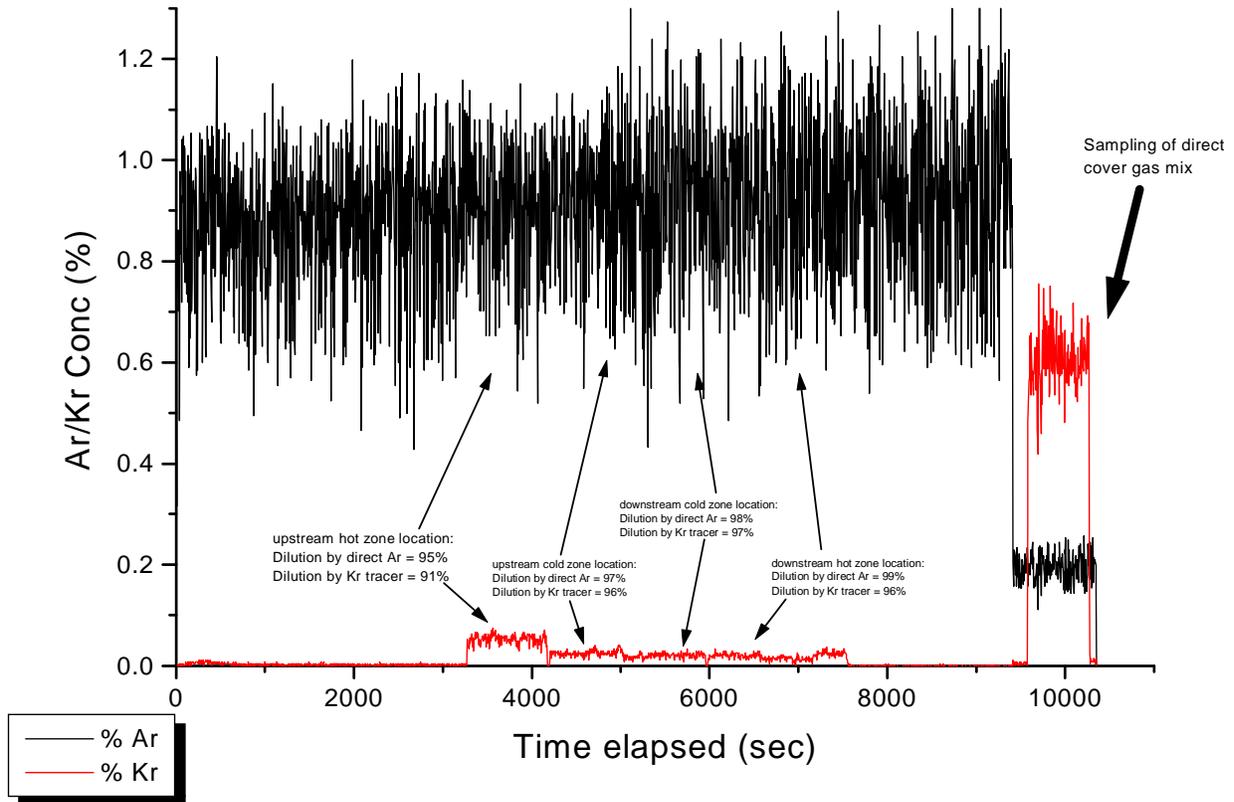**Figure 4-2.   RGA Dilution Measurements, 12 September 2007**

Figure 4-3.   RGA Dilution Measurements, 13 September 2007

DP calculations were carried out accordingly.

- For krypton tracer,

$$DP = 100 \times \left[1 - \frac{\text{sample krypton (\%)}}{\text{direct krypton in cover gas mixture (\%)}} \right].$$

- For argon intrusion, the calculations were more complex because the levels of argon native in the ambient air[7] and already present in the cover gas mixture from blended CDA must be considered. The equation below should be solved for DP.

$$\textit{sample } \arg on\, (\%) = \frac{DP}{100}\, x\, (\arg on\ in\ ambient\ air, 0.9332\%^{\,7}) + \left[\left(1 - \frac{DP}{100}\right) x\, (\arg on\ direct\ from\ \cov er\ gas\ (\%)) \right].$$

---

[7] S. Y. Park, et al., *Metrologia* **41,** 387-395 (2004)

The DP values at each location are reported in Table 4-1 along with their measurement uncertainties. Uncertainties were derived based on the measurement standard deviations across each monitoring period, which was assumed to take into account intermediate sampling errors and analytical measurement variability since the casting process was run in a steady state. There may also be inherent sampling variability due to ingot mold movement through the casting hood and interactions with flows from cover gas nozzles. The standard deviations were propagated throughout the DP calculation to produce the absolute measurement uncertainties listed in Table 4-1. The differences between DP values determined by krypton tracer and those determined by argon intrusion were similar to measurement uncertainties.

Table 4-1. Dilution Percentages (DP) Calculated by Kr Tracer and Direct Ar Monitoring

Calculation Method	Date	hu DP (percent)	cu DP (percent)	hd DP (percent)	cd DP (percent)
Kr Tracer	9/11/2007	86%(13)	98%(20)		
	9/12/2007	91%(16); 91%(17)	97%(21)	96%(24)	
	9/13/2007	91%(17)	96%(21)	96%(23)	97%(25)
Direct Ar	9/11/2007	83%(16)	95%(18)		
	9/12/2007	87%(21); 94%(23)	98%(25)	90%(23)	
	9/13/2007	95%(20)	97%(20)	99%(22)	98%(23)

Parenthetical values represent (±) one absolute standard deviation.

Dilution percentages were also calculated using the concentrations measured directly at the cover gas mixing point and the concentrations measured during noncasting conditions. DP values calculated by this method are presented in Table 4-2 and used the following equation:

$$DP = 100 - \left[\frac{noncasting\ feed\ gas\ conc.\,(ppmv)}{direct\ feed\ gas\ conc.\,(ppmv)} \right].$$

Dilution estimates obtained using the direct and noncasting approach were used as the primary factor for estimating dilution. For tests where this approach was not available due to a lack of data, an average DP was created for each sampling point using the noncasting and Kr tracer results. It should be noted that the results across the different dilution estimation approaches are relatively consistent.

Table 4-2. Dilution Percentages (DP) Calculated from Noncasting and Direct Concentrations

Test	hu (percent)	cu (percent)	hd (percent)	cd (percent)
1	86%(1)	94%(1)	-	-
2	83%(1)	94%(1)	-	-
3	-	-	-	-
4	89%(1)	96%(1)	-	-
5	-	-	97%(1)	98%(1)
6	-	-	-	-
7	92%(1)	86%(1)	-	-
8	-	-	-	-
9	-	-	-	-

"-" Indicates that either noncasting or direct concentration values are missing for that specific test and sample point. Parenthetical values represent (±) one absolute standard deviation.

4.2. Determining Cover Gas Destruction

Table 4-3 presents the cover gas flow rate, delivery concentration, FTIR measured concentration, dilution factor, and calculated DF value for each available sampling site for each cover gas test. A noncasting run was not possible for one of the Novec™ 612 mixtures runs on 12 September 2007. For SO_2, a noncasting run was not conducted because of logistical reasons. A direct sample of the SO_2 cover gas composition was also not possible from the temporary setup used during processing, so the direct SO_2 concentrations were estimated by calculation from the mass flow controller settings on the gas blending system. Average DF values for the SF_6, Novec™ 612, and SO_2 cover gas mixtures were 5 percent, 9 percent, and 39 percent, respectively.

Determining DF values involved several experimental measurements to derive concentrations and DP values. Each experimental measurement was subject to indeterminate uncertainty and contributed to the indeterminate error of the final results. The errors were propagated from measurements to final results by common rules that were derived from the total differentiation (by sum of all partials) of the DF equations discussed at the beginning of Section 4.[8] As will be discussed in Section 5, the DF values determined by dilution considerations carry significant uncertainties because the DP values are rather large and contain significant variance. This variance resulted in the generation of negative destruction values in some cases because the destruction is very low and approaching zero. For the sake of clarity, the negative destruction values are withheld from this report. The average destruction values presented are therefore only based on the positive results calculated using this methodology.

---

[8] D. Skoog, Principles of Instrumental Analysis, 3rd Ed., CBS College Publishing, 1985

Table 4-3. Percent Destruction for Cover Gas Testing

Test # (site)	Cover Gas Mixture Components	Flow[a] (lpm)	Cover Gas Delivery Conc. (ppmv)	Cover Gas Measured Conc. (ppmv)	Dilution Percentage[c] (percent)	Estimated Cover Gas Destruction Factor (percent)
1hu	SF_6/SO2/CDA/CO2	270	10,675	1,407	86%	4%
1cu	SF_6/SO2/CDA/CO2	135	10,675	572	94%	8%
2hu	SF_6/SO2/CDA/CO2	198	7,554	1,251	83%	3%
2cu	SF_6/SO2/CDA/CO2	99	7,554	456	94%	7%
3hu	SF_6/SO2/CDA/CO2	270	8,463	1,232	*89%*	≈0%
3cu	SF_6/SO2/CDA/CO2	135	8,463	640	*94%*	≈0%
3hd	SF_6/SO2/CDA/CO2	270	8,463	424	*96%*	≈0%
3cd	SF_6/SO2/CDA/CO2	135	8,463	333	*98%*	≈0%
4hu	Novec™ 612/CDA/CO_2	189	2,000	219	89%	≈0%
4cu	Novec™ 612/CDA/CO_2	95	2,000	77	96%	≈0%
5hd	Novec™ 612/CDA/CO_2	189	1,500	47	97%	≈0%
5cd	Novec™ 612/CDA/CO_2	95	1,500	27	98%	10%
6hu	Novec™ 612/CDA/CO_2	191	1,102	96	*89%*	23%
6cu	Novec™ 612/CDA/CO_2	96	1,102	161	*94%*	≈0%
6hd	Novec™ 612/CDA/CO_2	191	1,102	37	*96%*	4%
6cd	Novec™ 612/CDA/CO_2	96	1,102	74	*98%*	≈0%
7hu	Novec™ 612/CDA/CO_2	189	1,663	131	92%	≈0%
7cu	Novec™ 612/CDA/CO_2	95	1,663	228	86%	5%
8hd	SO_2/CDA	191	10,000	277	*96%*	22%
8cd	SO_2/CDA	95	10,000	128	*98%*	49%
9hu	SO_2/CDA	191	12,000	946	*89%*	30%
9cu	SO_2/CDA	96	12,000	296	*94%*	56%

[a] Approximate, estimated by reading flow rates on gas delivery manifold rotameters (uncalibrated). 2/3 of flow went to the hot zone and 1/3 to the cold zone.

[c] The dilution factor presented here comes from the noncasting/direct DP calculation for each specific test. When this value was unavailable, the averaged value of all DP values (except those determined by the Direct Ar method) for the designated sampling point was used and is presented in *italics*.

5. Discussion

5.1. Cover Gas Test Observations

Compared to the die casting crucibles previously studied, the design of typical magnesium ingot casting hoods suggested that the cover gas destruction would be low and difficult to estimate due to increased ambient air dilution and variability. This assumption was made due to the four leading factors listed below.

1. The overall surface area of molten magnesium to be covered in an ingot caster is smaller than typical die casting crucibles. Assuming that about six ingot molds containing molten metal are within the hot zone at the same time, and given that each mold has a surface area of about 800 cm^2, the total surface area of the covered molds is about 4,800 cm^2. A 1.2 meter diameter die casting crucible has a surface area of about 12,000 cm^2. A smaller covered surface area means that less of the cover gas concentrations are being consumed on a percentage basis than with a larger covered surface area.

2. The freshly poured ingots within the hot zone begin cooling immediately after injection of molten magnesium. Alloying crucibles and holding furnaces must keep the metal in a liquid state throughout processing. This implies that less cover gas will interact and break down at the ingot surface as it cools, leading to lower destruction rates.

3. The casting hood volumes are greatly affected by ambient air dilution. Excessive dilution makes differential measurements difficult to carry out because the amount of dilution must be precisely and consistently characterized.

4. The casting hood volumes are quite large and the ingot protection atmosphere is very turbulent due to high cover gas flow rates and movement of the ingot molds. These characteristics create difficulties for continuous real-time extraction of representative gas samples, which makes analytical measurement precision challenging and greatly influences destruction calculations.

These factors were born-out in the actual measurement results. Several reasonable estimations and observable trends can be gleaned from the results reported in Section 4. These observations would include the following:

- Destruction was generally low under all cases, with the exception of SO_2, which exhibited the highest destruction percentages (39 percent).
- The casting-versus-noncasting destruction determinations carry significantly lower measurement uncertainties and better reproducibility at each sampling location than do the destruction values determined by dilution, where some test cases yielded unrealistic negative values.

- As expected, the most consistently reliable destruction percentages for both measurement methods were calculated at the upstream hot zone sampling location.

For measurements during ingot casting, this study yields the following primary recommendations for future research: (1) maximize the representativeness of concentration analysis by setting up as many sampling points as possible for simultaneous gas extraction from the casting hood, and then (2) characterize ambient air dilution effects by basing the destruction calculations upon casting-versus-noncasting conditions. The extent to which (1) can be applied is highly dependent upon logistical and process concerns. For this study it was not feasible to set up more than two sampling ports per casting hood zone without interfering with process activities such as metal pouring, ingot skimming, and conveyor belt operation. An additional recommendation is to account for air turbulence effects during monitoring periods. For example, extend casting and noncasting events over longer continuous blocks of time to help smooth out the averaging and subsequent comparison of concentrations during the casting-versus-noncasting conditions.

One benefit of the low destruction values and excessive air dilution is that the concentrations of cover gas byproducts were often negligible within the casting hood and, by extension, also within the operator room environment. The tables in Section 3 indicate that the only measurable byproduct was HF and its average concentrations were almost always under 1 ppmv. As expected, Novec™ 612 usually produced slightly more HF than SF_6/SO_2, but no other fluorinated species (including PFIB) were detected.

This study also indicates that there is significant uncertainty regarding the exact mixture of cover gas being applied using the current rotameter-based control system. Measured cover gas mixture concentrations for SF_6 and SO_2 from direct FTIR sampling at the manifold were significantly higher than what was expected based on rotameter readings that controlled the mixture. Monitoring of the cover gas system currently utilized at the facility indicates that there may be significant over-protection occurring and that optimization to minimize cover gas usage would be achievable if the current rotameter-based control system was replaced.

It should also be noted that the SF_6/SO_2 cover gas system is unique in that there are two reactive cover gas constituents present. The exact nature of how this impacts the destruction of SF_6 is unclear. It is possible that a SF_6-only cover gas system used in this application would produce different results for destruction and byproduct formation.

5.2. Climate Change Potential Discussion

One of the benefits of using Novec™ 612 and SO_2 as cover gases for magnesium melt protection is their contribution to global climate change is significantly lower when compared to SF_6. This is evident when comparing their estimated global warming potentials (GWPs). Table 5-1 presents GWPs of several compounds detected during this study.

Table 5-1. Comparison of 100-Year GWP Estimates from the Intergovernmental Panel on Climate Change (IPCC) Fourth (2007) Assessment Report

Gas	IPCC GWP
Methane	25
Nitrous Oxide	298
Sulfur Hexafluoride (SF_6)	22,800

IPCC (2007), Climate Change 2007: The Scientific of Climate Change. Intergovernmental Panel on Climate Change, Cambridge University Press. Cambridge, U.K.

The ingot casting area contains a variety of compounds, but only those with corresponding GWP values were used in estimating the overall GWP impact of switching to alternate cover gases. This calculation consisted of multiplying the average concentrations (parts per million by volume) for each of the component cover gases and applicable destruction products, by their respective GWP factors (obtained from the Second Assessment Report of the Intergovernmental Panel on Climate Change) to obtain a GWP-weighted value. The summation of all the GWP-weighted values for a particular cover gas resulted in the normalized CO_2 equivalent, which was compared to the CO_2 equivalent corresponding to SF_6.[9]

Table 5-2 shows that when comparing the normalized CO_2 equivalent, or composite GWP, the alternate cover gases have a much lower impact. An obvious source for this reduction can be found in the incredibly high GWP of SF_6 shown in Table 5-1. Novec™ 612's GWP has not been supplied by the IPCC, but is likely to be extremely low (i.e., Novec™ 612 is a fluorinated ketone, which is assumed to have an atmospheric lifetime of approximately 5 days and a GWP on the order of 1).[10] SO_2 is not an IR absorber and therefore has no global warming potential. Compared to using SF_6, switching to Novec™ 612 produces a reduction in overall global warming impact of at least 99.7 percent.[11] Changing the cover gas from SF_6 to SO_2 reduces the global warming impact by at least 99.9 percent but introduces a more complex operational scenario due to toxicity concerns.

The above comparison does not include the specific flow rates for each cover gas. In order to provide a more comprehensive analysis of composite GWP, an additional comparison was conducted. Using the ideal gas law, the molecular weights of each gas and the delivery flow

---

[9] Fugitive SF_6 and CH_4 concentrations were excluded from the overall GWP calculations for the cover gases.

[10] D'Anna B, Sellevag S.R., Wirtz K., and Nielsen C.J. Photolysis Study of Perfluoro-2-methyl-3-pentanone Under Natural Sunlight Conditions Environ Sci and Tech 2005 39(22) 8708-8711

rate of the cover gas was used to estimate the composite emission rate in grams per hour (g/hr). This equation can be described as follows:

$$Emission\ Rate\left(\frac{grams}{hour}\right) \ = \ ppmv \times MW \times lpm \times \frac{60\ \min}{hour} \div \left(38.6\ liters\,/\,mole \times 10^{6}\right)$$

      ppm = measured average concentration in parts per million
      MW = molecular weight in grams per mole
      lpm = gas flow in liters per minute

These values were summed to provide a composite GWP value that was weighted by the cover gas flow rate. The average flow weighted GWP values were then compared against the corresponding values for the SF_6/SO_2 system. Based on this approach, both of the cover gas alternatives were observed to reduce GHG emissions by at least 99.9 percent relative to SF_6/SO_2 system. This result is also bourn out when comparing individual tests, such as Test 3 and 6; averaging the results for the four monitoring points in each test results in a reduction in GHG emissions of more than 99.9 percent. Details of the flow-weighted GHG emission impacts are presented in Table 5-3.

5.3. Uncertainty Discussion

The results of this measurement study should not be interpreted to represent an absolute analysis of GHG emissions associated with Novec™ 612, SO_2, and SF_6 cover gas usage. While this study does present a relatively accurate measurement analysis and approximate comparison of GHG emissions, there are several areas of uncertainty inherent with this methodology. These areas of uncertainty include FTIR and RGA error, error associated with blending gases, dilution correction, and analytical and operational variation of the ingot casting machine evaluated. The high levels of dilution – on the order of 90 percent – results in significant uncertainty associated with destruction estimates.

Measurements taken by the FTIR and RGA are subject to variability inherent with highly complex analytical equipment. While all prudent steps were taken during the measurement study to minimize this contributor to uncertainty (see Section 2 and Appendix A), a small degree of error is unavoidable.

---

[11] Please refer to Section 5-3 for a discussion regarding the uncertainty associated with this methodology.

Table 5-2. Normalized GWP Comparison of Measured Emissions from Inside the Casting Hood

Test # (site)	Cover Gas Mixture Components	Cover Gas Delivery Conc.[a] (ppmv)	Measured Cover Gas Conc. (ppmv)	GWP Weighted Cover Gas[b]	GWP Weighted CO_2	GWP Weighted CH_4	GWP Weighted SF_6	Normalized CO_2 Equivalent[c]	Average by Cover Gas	Chg from SF_6 (percent)
1hu	SF_6/SO_2/CDA/CO_2	10,675	1,407	32,083,235	64,180	*95*	*0*	32,147,415		
1cu	SF_6/SO_2/CDA/CO_2	10,675	572	13,042,073	26,674	*95*	*0*	13,068,748		
2hu	SF_6/SO_2/CDA/CO_2	7,554	1251	28,515,105	71,212	*66*	*0*	28,586,318		
2cu	SF_6/SO_2/CDA/CO_2	7,554	456	10,405,526	21,135	*65*	*0*	10,426,661	18,038,815[d]	
3hu	SF_6/SO_2/CDA/CO_2	8,463	1232	28,089,380	68,095	*1,403*	*0*	28,157,476		
3cu	SF_6/SO_2/CDA/CO_2	8,463	640	14,581,075	26,374	*2,069*	*0*	14,607,449		
3hd	SF_6/SO_2/CDA/CO_2	8,463	424	9,673,990	29,109	*81*	*0*	9,703,100		
3cd	SF_6/SO_2/CDA/CO_2	8,463	333	7,594,120	19,233	*67*	*0*	7,613,353		
4hu	Novec™ 612/CDA/CO_2	2,000	219	219.3	78,066	*93*	*14,666*	78,285		
4cu	Novec™ 612/CDA/CO_2	2,000	77	76.9	25,915	*129*	*18,084*	25,992		
5hd	Novec™ 612/CDA/CO_2	1,500	47	47.0	23,956	*92*	*14,518*	24,003		
5cd	Novec™ 612/CDA/CO_2	1,500	27	27.0	13,137	*133*	*19,682*	13,164		
6hu	Novec™ 612/CDA/CO_2	1,102	96	95.6	66,593	*53*	*2,450*	66,689	51,950	99.7%
6cu	Novec™ 612/CDA/CO_2	1,102	161	161.4	91,743	*186*	*11,385*	91,905		
6hd	Novec™ 612/CDA/CO_2	1,102	37	37.5	32,158	*1,777*	*3,639*	32,195		
6cd	Novec™ 612/CDA/CO_2	1,102	74	73.8	49,905	*3,480*	*22,514*	49,979		
7hu	Novec™ 612/CDA/CO_2	1,663	131	131.4	52,494	*45*	*1,794*	52,626		
7cu	Novec™ 612/CDA/CO_2	1,663	228	228.5	84,434	*173*	*6,474*	84,663		
8hd	SO_2/CDA	10,000	277	0	22,754	*91*	*8,545*	22,754		
8cd	SO_2/CDA	10,000	128	0	9,905	*80*	*11,086*	9,905	10,919	99.9%
9hu	SO_2/CDA	12,000	946	0	10,585	*85*	*6,981*	10,585		
9cu	SO_2/CDA	12,000	296	0	434	*86*	*8,061*	434		

[a] Measured directly at cover gas manifold

[b] GWP weighting based on dilution corrected concentration for the primary cover gas constituent (e.g., Novec™ 612, SF_6)

[c] Please note that the normalized equivalent values exclude fugitive CH_4 and SF_6 emissions which are reported in *italics* for completeness.

[d] SF_6 composite GWP baseline estimate for comparison with other tests.

Table 5-3. GWP (Weighted by Cover Gas Flow) Comparison of Measured Emissions from Inside the Casting Hood

Test # (site)	Cover Gas Mixture Components	Cover Gas Delivery Conc.[a] (ppmv)	GWP Weighted Cover Gas[b] (g/hr)	GWP Weighted CO_2 (g/hr)	GWP Weighted CH_4 (g/hr)	GWP Weighted SF_6 (g/hr)	Normalized CO_2 GWP Equivalent[c] (g/hr)	Average by Cover Gas (g/hr)	Chg from SF_6 (percent)
1hu	SF_6/SO_2/CDA/CO_2	10,675	1,966,281	1,185	*1*	*0*	1,967,466	860,144[d]	
1cu	SF_6/SO_2/CDA/CO_2	10,675	399,654	246	*0*	*0*	399,900		
2hu	SF_6/SO_2/CDA/CO_2	7,554	1,280,759	964	*0*	*0*	1,281,723		
2cu	SF_6/SO_2/CDA/CO_2	7,554	233,683	143	*0*	*0*	233,826		
3hu	SF_6/SO_2/CDA/CO_2	8,463	1,722,714	1,259	*9*	*0*	1,723,972		
3cu	SF_6/SO_2/CDA/CO_2	8,463	447,127	244	*7*	*0*	447,370		
3hd	SF_6/SO_2/CDA/CO_2	8,463	593,303	538	*1*	*0*	593,841		
3cd	SF_6/SO_2/CDA/CO_2	8,463	232,873	178	*0*	*0*	233,050		
4hu	Novec™ 612/CDA/CO_2	2,000	20	1,010	*0*	*629*	1,030	480	99.9%
4cu	Novec™ 612/CDA/CO_2	2,000	4	168	*0*	*388*	171		
5hd	Novec™ 612/CDA/CO_2	1,500	4	310	*0*	*623*	314		
5cd	Novec™ 612/CDA/CO_2	1,500	1	85	*0*	*422*	86		
6hu	Novec™ 612/CDA/CO_2	1,102	9	871	*0*	*106*	880		
6cu	Novec™ 612/CDA/CO_2	1,102	8	600	*0*	*247*	607		
6hd	Novec™ 612/CDA/CO_2	1,102	4	421	*8*	*158*	424		
6cd	Novec™ 612/CDA/CO_2	1,102	3	326	*8*	*488*	330		
7hu	Novec™ 612/CDA/CO_2	1,663	12	679	*0*	*77*	691		
7cu	Novec™ 612/CDA/CO_2	1,663	11	546	*0*	*139*	557		
8hd	SO_2/CDA	10,000	0	297	*0*	*370*	297	126	99.9%
8cd	SO_2/CDA	10,000	0	65	*0*	*240*	65		
9hu	SO_2/CDA	12,000	0	138	*0*	*303*	138		
9cu	SO_2/CDA	12,000	0	3	*0*	*175*	3		

[a] Measured directly at cover gas manifold

[b] GWP weighting based on dilution corrected concentration for the primary cover gas constituent (e.g., Novec™ 612, SF_6)

[c] Please note that the normalized equivalent values exclude fugitive CH_4 and SF_6 emissions which are reported in *italics* for completeness.

[d] SF_6 composite GWP baseline estimate for comparison with other tests.

Appendix A – Calibrations and Diagnostic Checks

This section summarizes the on-site FTIR/RGA calibration and diagnostic procedures carried out before and during the sampling tests.

A.1. FTIR Calibrations and System Checks

A series of on-site calibration and system checks was performed on each FTIR and respective sampling system prior to testing to ensure data quality. These checks are described in the remainder of this Section.

A.1.1. FTIR Sample Cell Integrity Checks

The integrity of each FTIR sample cell was confirmed prior to sampling by (1) drawing a terminal vacuum of < 200 torr, then (2) sealing off the sample cell while still under vacuum, then (3) monitoring any pressure rise (i.e., leak rate) within the cell by observing its pressure transducer reading over a several-minute period. A cell was considered leak-tight when a leak rate of < 2 torr min^{-1} was observed. The evacuated pressure on each FTIR sample cell (hot zone system, cold zone system, and worker exposure system) did not rise above measurable values over a 1-min period.

A.1.2. Infrared Detector Linearity Checks

For best results, the IR detector in each FTIR system must yield a linear response throughout the measurement absorbance ranges within the measurement frequency range of all sample spectra. A software linearizer was used to continuously adjust the MCT detector preamp signal to achieve the desired linear response. To optimize the linearizer, background spectra were acquired with and without a polystyrene film in the IR beam. Comparison of the strongly absorbing polystyrene bands in the low-, mid-, and high-frequency regions against a clean background enables the processor to appropriately set the linearizer terms (offset, linear, quad, cubic, and delay). This procedure was run prior to the start of testing for each FTIR, and subsequent spectra were periodically visually checked to confirm that linearity was maintained.

A.1.3. Noise Equivalent Absorbance (NEA, or Signal-to-Noise Ratio) Tests

NEA tests provide a measure of system noise – more specifically, the sensitivity of the instrument at the specified spectral resolution (in this case, 0.5 cm^{-1}) and number of co-added spectra (in this case, 256, or 2 min of signal averaging). A two-min FTIR spectral background was recorded while the sample cell was purged with dry nitrogen. A subsequent "sample" spectrum was recorded while the cell was still under nitrogen purge immediately after the background recording. The two spectra were ratioed to provide a snapshot of instrumental noise. The NEAs of all three FTIR systems were well below 0.001 absorbance units across all

measurement frequencies prior to sampling, which enabled instrument-limited quantitative analysis sensitivities of < 1 ppmv to be achieved for all compounds of interest.

A.1.4. Path Length

The sample cells utilized for this study were geometrically fixed with an FTIR cold zone system path length of 20.1 m and a hot zone system path length of 5.11 m. The worker exposure FTIR system contained an adjustable multi-pass White cell that was aligned, set, and calibrated at a path length of 10 m.

A.1.5. Spectrometer Frequency and Resolution Checks

A real-time check of frequency position and resolution was performed at each FTIR prior to and directly following each round of testing. These checks were performed by monitoring a specific water absorption band present in ambient air. The position of this line must not deviate more than $\pm$ 0.005 cm^{-1} from the reference value over the course of each test. Likewise, the linewidth of this band, which is directly related to instrument resolution, must not deviate more than $\pm$ 0.05 cm^{-1} from the reference value over the course of each test.

A.1.6. Spectral Background

A spectral background is essentially a "blank spectrum" in that it does not contain any of the target compounds normally present in the sample. It was created by purging each cell with ultra-high-purity (UHP) nitrogen while recording a spectrum. This spectrum was then used by the analytical software to ratio against each sample spectrum to produce an absorbance spectrum for quantitative analysis. A new spectral background was generated each day prior to testing.

A.1.7. Sample Cell Exchange Rate

With sampling flow rates on the order of 5 L min^{-1} through each cell, complete sample exchanges took approximately 7 s for the 5.11 m cell, 18 s for the 20.1 m cell, and 30 s for the 10 m worker exposure cell, which had the largest internal volume. Since spectral signal averaging was performed over 2-min intervals, each recorded spectrum represented an integrated average over multiple sample cell exchanges.

A.2. RGA Calibrations and System Checks

A series of on-site calibration and system checks was performed on the RGA and sampling system prior to and during sampling to ensure high data quality. These checks and calibrations are described in the remainder of this Section.

A.2.1. Sample Inlet and Mass Analyzer Chamber Pressures

Pressure was continuously monitored in the mtorr range via a thermocouple gauge within the sample inlet chamber, which is considered to be the high pressure side of the chamber

aperture (see block diagram, Figure 2-2). The sample inlet chamber was directly interfaced to the venturi pump-driven sample extraction line. The venturi pumping speed and valve orifice maintained a constant pressure of 5 x 10^{-2} torr within the sample inlet chamber. Given a fixed chamber aperture previously installed at URS, the 5 x 10^{-2} torr constant sample inlet chamber pressure created a 5 x 10^{-4} torr total pressure within the mass analyzer chamber. Pressures were continuously monitored by cold cathode gauge. When isolated from the sample inlet, total background chamber pressures (~5 x 10^{-6} torr) were two orders of magnitude less than this mass analyzer chamber total pressure. These pressures allowed RGA sensitivities for argon of ~100 ppmv at m/e = 40, as previously mentioned in Section 2.2.2. The partial background pressures observed for krypton at m/e = 84 were about half an order of magnitude lower than those observed for argon at m/e = 40 (~5 x 10^{-7} torr versus ~1 x 10^{-6} torr), so the detection limit for krypton was expected to be less than the 100-ppmv sensitivity noted for argon.

A.2.2. RGA Response Calibrations for Argon and Krypton

RGA responses at the mass analyzer channels corresponding to m/e = 40 and m/e = 84 were calibrated on two separate occasions (11 September 2007 and 13 September 2007) against known concentrations of argon and krypton, respectively. Pure argon and krypton gases were mixed with UHP nitrogen at precision flows delivered by mass flow controllers. The mixture was sent to the sample inlet venturi pump under the same flow and orifice settings as when field samples were collected. The calibration curves displayed in Figures A-1 and A-2 were fit to the detector signal and expressed as the ratio of partial pressure (percentage of total chamber pressure at m/e = 40 or 84) to concentration (percentage). The curves were mainly linear at lower concentrations with some nonlinearity at higher concentrations; therefore, they were fit to second order polynomials with relatively small quadratic coefficients. The polynomials did not differ a great deal between the first and second calibrations for each compound, so the calibration curves produced on 11 September 2007 were applied to sample scans collected on 11-12 September 2007, whereas the calibration curves produced on 13 September 2007 were applied to sample scans collected on 13-14 September 2007.
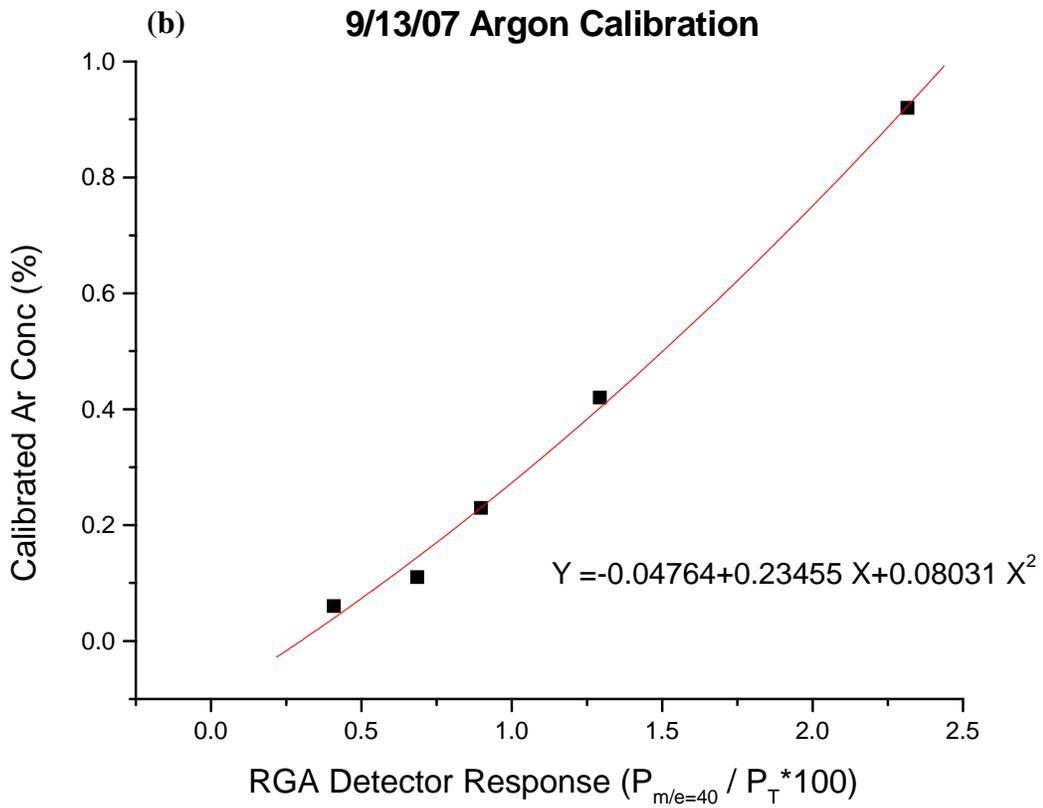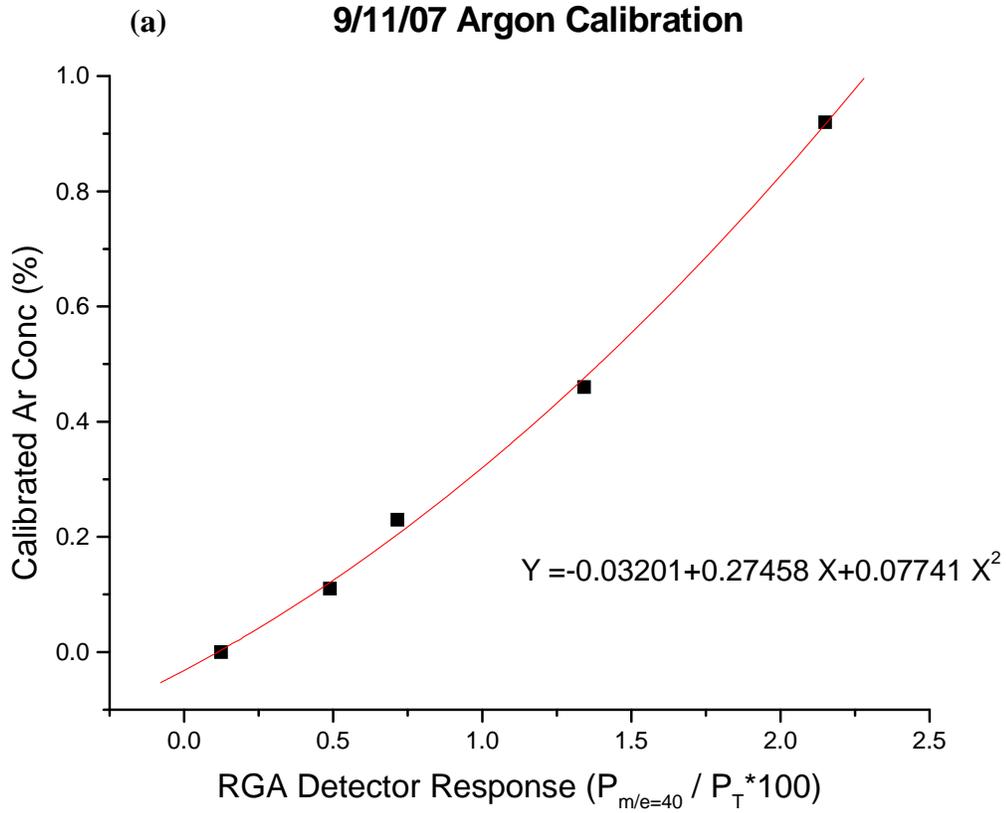
(a) **9/11/07 Argon Calibration**

Calibrated Ar Conc (%)

$Y = -0.03201 + 0.27458\ X + 0.07741\ X^2$

RGA Detector Response $(P_{m/e=40} / P_T \ast 100)$

(b) **9/13/07 Argon Calibration**

Calibrated Ar Conc (%)

$Y = -0.04764 + 0.23455\ X + 0.08031\ X^2$

RGA Detector Response $(P_{m/e=40} / P_T \ast 100)$

Figure A-1.   Calibrated RGA Response for Argon

(a) **9/11/07 Krypton Calibration**

Calibrated Kr Conc (%)

$Y = -0.01678 + 0.35308\,X + 0.03926\,X^2$

RGA Detector Response ($P_{m/e=84}$ / P_T*100)

(b) **9/13/07 Krypton Calibration**

Calibrated Kr Conc (%)

$Y = -0.02032 + 0.26523\,X + 0.12842\,X^2$
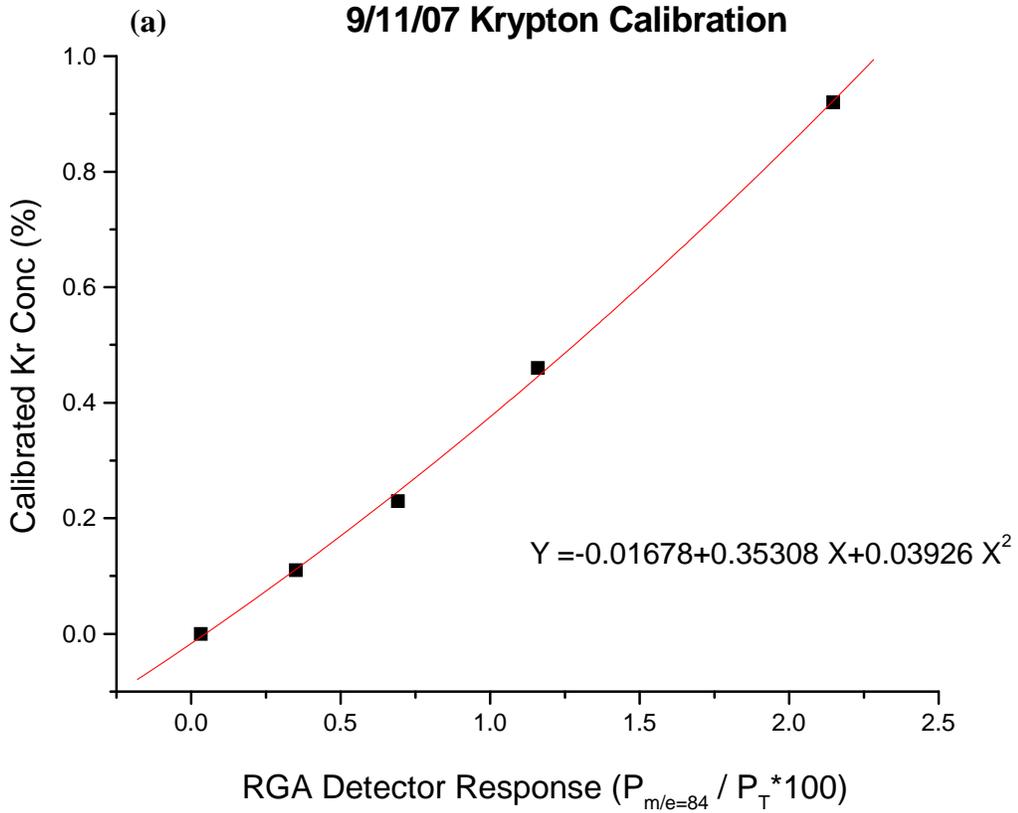
RGA Detector Response ($P_{m/e=84}$ / P_T*100)
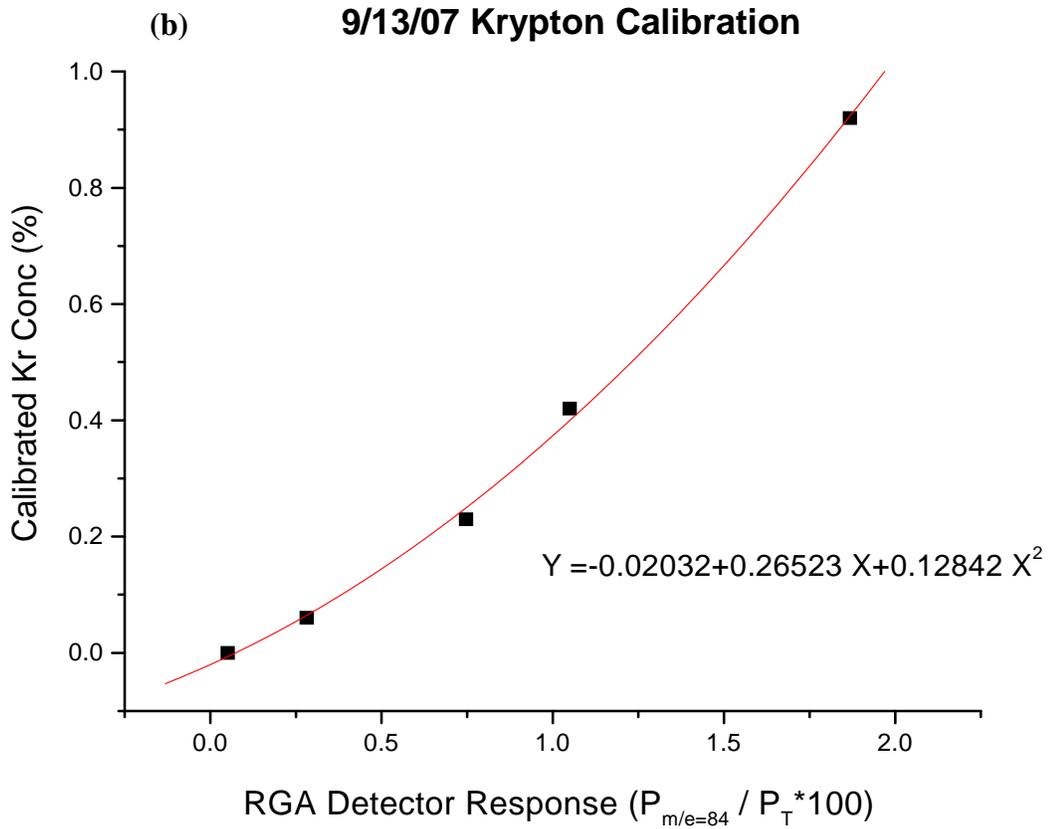
Figure A-2.   Calibrated RGA Response for Krypton

Appendix B – Measurement Study Protocol

The analytical measurement and data interpretation approach described herein attempts to determine, by empirical means, the most conservative cover gas destruction possible for a given type of magnesium process tool and gas flow ranges used during production. This approach is based on the experience from the MagReTech study and pertains to only those processes that can allow typical operation and cover gas flow without molten metal in place, as well as normally with molten metal. Therefore, ingot casting and chilling machines are prime candidates for this approach, as opposed to alloying and die casting crucibles which are often kept under constant high temperatures and filled with metal. The approach encompasses all the measurement variance brought about by the process gas flows (including turbulence invoked by ambient air dilution) in conjunction with analytical instrument and sampling variability. The variances associated with each measurement condition needed in calculating the degradation factor are then properly propagated through the calculations to the final result. The maximum destruction factor is thus considered by adding the propagated variance to the final calculation result. If the process under study is normally run over a range of cover gas concentrations, this measurement approach is to be conducted at both the lowest concentration and highest concentration of that range; the reportable maximum destruction factor is then the greater of the two.

The Test Plan outlines how the experimental observables and variances needed to determine the maximum degradation factors are obtained. The Quantitative Data Analysis section describes how the measurements are used to estimate destruction factors and how the variances are propagated. A hypothetical example is provided to help illustrate the measurement approach.

Test Plan

1. Set up a real-time measurement instrument to continuously extract and analyze a low volume slipstream of the completely blended cover gas mixture prior to injection into the melt protection area. The extractive analysis technique should not significantly impact the overall gas flow within normal process operations, and allow enough consecutively recorded measurements as to be statistically relevant. For instance, an extractive FTIR system monitoring SF_6 concentrations over one-minute of signal averaging will produce 240 data points within a four-hour continuous sampling period.

2. Set up a second real-time measurement instrument to continuously extract and analyze a low volume stream of cover gas within the process environment (i.e., where molten magnesium is to be covered during casting or chilling). The extractive analysis technique at this sample location should not significantly impact the overall gas flow throughout the process environment, should allow the most representative sampling configuration possible (for instance, equidistant perforated sample probes that traverse the entire width of process head space a few centimeters from the molten metal surfaces), and also allow enough consecutively recorded measurements as to be statistically relevant. This instrument will be sampling coincidentally with the instrument described in step #1, so the implementation of two identical analysis techniques (for instance, two extractive FTIR systems) is ideal.

3. *With molten magnesium present during production*: Simultaneously monitoring both sampling locations over a sufficiently long time period will produce a mean concentration during metal production at the point of cover gas injection, MP^i, and a mean concentration during metal production within the process environment, MP^e. Also, the 99 percent confidence level of both means, which when expressing as +/- values about the means would contain virtually all sources of indeterminate measurement error, can be estimated as 2.58 times the standard deviations (divided by the square root of the number of measurements) of their respective data sets. Hence, the experimentally determined MP^i / MP^e would carry associated $\sigma_{MP}{}^i / \sigma_{MP}{}^e$ as total measurement uncertainties (the squares of which being measurement variances) to be considered when calculating degradation percentages.

4. *With molten magnesium not present during mock production*: Simultaneously monitoring both sampling locations under the same configurations and over a similar length of time as conducted in step #3 will produce, under nonmetal process conditions, an experimentally determined NP^i / NP^e pair and associated $\sigma_{NP}{}^i / \sigma_{NP}{}^e$ measurement uncertainties. These are needed to effectively estimate the amount of ambient air dilution present in an open process.

5. Steps #3 and #4 are to be repeated as necessary over the cover gas concentration ranges utilized during normal production, presumably since the degradations may be significantly different depending on mixture ratios. This typically means an experimental

pair will be run at the lowest and the highest operating concentration, with the highest destruction percentage reported to be conservative.

6. Standard analytical measurement protocols, pertaining to the technique of choice, must be run to characterize instrumental accuracy and reproducibility for each experiment (in effect, any determinate errors associated with the instruments are quantified). Typically, this means a pre-test and post-test calibration run for all instruments to ensure accurate and consistent measurements at both sampling locations for each metal/nonmetal test condition.

Quantitative Data Analysis

- For the noncasting sampling period, the reduction of injected cover gas concentrations represents only the ambient air dilution in the system because molten magnesium is not present to react with the cover gas. Therefore,

$$Dilution = 1 - \frac{NP^e}{NP^i}$$

- For the casting or metal present sampling period, the reduction of injected cover gas concentrations represents the ambient air dilution *plus* destruction in the system, for molten magnesium is present. Therefore,

$$[Degradation + Dilution] = 1 - \frac{MP^e}{MP^i}$$

- To determine solely the destruction factor, DF:

$$DF = [Degradation + Dilution] - Dilution = \frac{NP^e}{NP^i} - \frac{MP^e}{MP^i} \qquad (1)$$

- Since the sum of relative variances for each ratio yields the relative variance of the result for each ratio in (1), and the sum of absolute variances for each term in (1) yields the absolute variance of the difference of terms[12], the variances of equation (1) can be propagated and simplified to produce the variance associated with the destruction factor:

$$\sigma_{DF}{}^2 = \left(\frac{\sigma_{NP^e}}{NP^i}\right)^2 + \left(\frac{NP^e \sigma_{NP^i}}{NP^{i2}}\right)^2 + \left(\frac{MP^e \sigma_{MP^i}}{MP^{i2}}\right)^2 + \left(\frac{\sigma_{MP^e}}{MP^i}\right)^2$$

Hence, the measurement uncertainty for DF is:

$$\sigma_{DF} = \left[\left(\frac{\sigma_{NP^e}}{NP^i} \right)^2 + \left(\frac{NP^e \sigma_{NP^i}}{NP^{i2}} \right)^2 + \left(\frac{MP^e \sigma_{MP^i}}{MP^{i2}} \right)^2 + \left(\frac{\sigma_{MP^e}}{MP^i} \right)^2 \right]^{1/2} \qquad (2)$$

Example

The noncasting sampling period produced mean SF_6 concentrations of 1000 ppmv and 500 ppmv for the cover gas injection point and process environment, respectively. The 99 percent confidence limit (basically, a multiple of the standard deviation) was 50 ppmv for each. The subsequent metal sampling period produced mean SF_6 concentrations of 1000 ppmv and 400 ppmv for the cover gas injection point and process environment, respectively. The 99 percent confidence limit was also 50 ppmv for each. To summarize,

NP^i = 1000 ppmv; $\quad \sigma_{NP^i}$ = ±50 ppmv

NP^e = 500 ppmv; $\quad \sigma_{NP^e}$ = ±50 ppmv

MP^i = 1000 ppmv; $\quad \sigma_{MP^i}$ = ±50 ppmv

MP^e = 400 ppmv; $\quad \sigma_{MP^e}$ = ±50 ppmv

The destruction factor, DF, for SF_6 can thus be computed via equation (1):

$$DF = \frac{NP^e}{NP^i} - \frac{MP^e}{MP^i} = \frac{500}{1000} - \frac{400}{1000} = 0.1$$

And the DF uncertainty is derived from (2):

$$\sigma_{DF} = \left[\left(\frac{50}{1000} \right)^2 + \left(\frac{500 * 50}{1000^2} \right)^2 + \left(\frac{400 * 50}{1000^2} \right)^2 + \left(\frac{50}{1000} \right)^2 \right]^{1/2} = 0.078$$

Meaning, the DF for SF_6 has been empirically determined as 10(±7.8) percent, so a conservative DF estimate of 17.8 percent would be considered.

---

[12] *Principles of Instrumental Analysis*, D. A. Skoog, 3rd Ed., 1985.